NASA CR-187116

High-Power Converters for Space Applications

Phase 1 Final Report and Phase 2 Plans

Contract NAS3-25800

Prepared for
NASA Lewis Research Center
Cleveland, Ohio

Prepared by
GE Corporate Research and Development
Schenectady, New York
and
Maxwell Laboratories, Inc.
San Diego, California

June 1991

90SRD008

TABLE OF CONTENTS

TABLE OF CONTENTS (Cont'd)

LIST OF ILLUSTRATIONS

LIST OF ILLUSTRATIONS (Cont'd)

LIST OF TABLES

ABSTRACT

Phase 1 of this program is a concept definition effort to extend space-type dc/dc converter technology to the megawatt level with an overall weight objective of less than 0.1 kg/kW (220 lb/MW), including components, structures, and cooling capability to interface with a heat rejection system. Two advanced power conversion system designs were evaluated for Phase 1 and both designs represent an extension of dc-to-dc converter technology to well beyond the present state of the art. Either design approach operates from a 5-kV energy source of stacked fuel cells and provides a voltage step-up to 100 kV at up to 10 A of current. This charges energy storage capacitors for pulse discharge at rates to 100 pps at a duty cycle of 17 min on, 73 min off. Both approaches use a full-bridge inverter having MCTs (MOS commutated thyristors) as the high-power, high-speed switching device. Also, both design approaches use gaseous hydrogen cooling and a proven crowbar fault protection scheme.

The GE-CRD system utilizes an advanced design high-voltage transformer/rectifier filter (ultra-low reflected ac capacitance) in series with a resonant tank circuit, driven by an inverter operating at high frequency (20 to 50 kHz) to minimize the size of inductive and capacitive components. Output voltage control is obtained through a combination of frequency and phase shift control. Fast transient response and stability is ensured through a special protocol called optimal control. Super-resonant operation (above the resonant frequency of the tank) employing MCTs provides the following advantages: lossless snubbing for switch protection, no turn-on switching loss, use of medium-speed inverter diodes, no di/dt limiting required, intrinsic current limiting under load-fault conditions. The estimated weight of the GE-CRD system is 88.5 kg, with an enclosed volume of 1.5 ft^3. Efficiency is estimated at 94.4% for a total system loss of 55.711 kW when operating at 1-MW load power. The GE-CRD system is based on technology developed for a product application and has demonstrated a high degree of reliability.

The Maxwell system is based on a resonance transformer approach developed at Maxwell Labs and avoids the use of a high-voltage transformer by combining a cascade of five LC resonant sections operated at a fixed frequency of 100 kHz. The 5-kV bus voltage is converted to a square wave by the inverter, stepped up to a 100-kV sine wave by the resonant action of the cascade of LC sections, and rectified and filtered. The inductors of the resonance transformer do not use magnetic cores, which reduces loss and weight. The Maxwell system has an estimated weight of 83.8 kg and an enclosed volume of 4.0 ft^3. Efficiency is estimated at 87.2% for a total system loss of 146.411 kW when operating at 1-MW load power.

Plans are given for Phase 2 work for the fabrication and testing of the dc/dc converters described in Phase 1.

Section 1

INTRODUCTION

1.1 Program Objectives

The objective of this NASA-Lewis Research Center contract with GE Corporate Research and Development and Maxwell Laboratories is to extend space-type dc/dc converter technology to the megawatt level, with an overall weight objective of less than 0.1 kg/kW (220 lb/MW) including components, structures, and cooling capability to interface with a heat rejection system. The converter will employ an inverter and a transformer (GE) or an inverter and a cascade of resonant L-C sections (Maxwell) to step-up the voltage from 5 kV dc to 100 kV dc. Present power converter principles must be extrapolated to simultaneously achieve the goals of high power and high voltage, with high-frequency operation for light weight. Typically, the input will be stacked fuel cells at a nominal voltage of 5000 V dc. It is expected that the loads supplied by the dc/dc converter will need up to 100 kV of steady output, or up to 10 A of current to charge energy storage capacitors for pulse discharge at rates up to 100 pulses per second. The operational duty cycle is considered to be 17 min (1000 s) on and 73 min off (90-min orbit).

1.2 Program Phases

The program has two phases:

Phase 1 – Concept definition (present phase)

Phase 2 – A. Build and test 100-kW "proof of principle" breadboard

B. Build and test 1-MW "proof of principle" breadboard

C. Build and test 1-MW brassboard

Phase 1 includes preliminary design work on two alternative dc-to-dc converter systems using different approaches. Based on comparative evaluation of the results, NASA may select one or both systems for further development in Phase 2. The two systems and the responsible contractors are

- Transformer-linked dc-to-dc converter – GE-CRD
- Transformerless voltage multiplier dc-to-dc converter – Maxwell Labs

For each system, the following have been accomplished in Phase 1:

1. Specification of components required for Phase 2.
2. Identification of research and development required for those components.
3. Estimation of size, weight, and efficiency.
4. Identification of partners, subcontractors, or vendors other than GE-CRD or Maxwell Laboratories to supply components and services in Phase 2.

Section 2

HIGH-VOLTAGE OPTICALLY CONTROLLED MCT SWITCH MODULE

2.1 Background

The MCT represents a new class of power switching devices. Its development was made possible by combining power MOS and power bipolar device concepts and process capability. Compared on a current handling basis, a 600-V MCT can conduct 1000 times and 50 times greater current than a 600-V V-FET or a 600-V IGBT, respectively, at a very low 1.5-V forward drop. The MCT's high switching speed coupled with its very low switching losses as well as its low forward drop make this the only device available at present with which to achieve the stringent goals for the present development.

Operation in the frequency range of 20 to 50 kHz is necessary at high efficiency to achieve the low weight goal of this program. To generate 1 MW of power using the series superresonant circuit topology approach operating from a 5-kV dc power source requires 10 series MCT modules in each of four bridge arms for a total 40 modules. Each MCT module developed in the present study is capable of turning off 330 A into 500 V while dissipating 760 W for the typical case. MCT modules can be paralleled for increased current and series connected to accommodate a wide range of dc bus voltages.

2.2 MCT Module Structure

2.2.1 Package Concept

A new approach to power device packaging termed the Hermetic Thin-Pak (HTP) has been developed at CRD. This package exhibits low electrical impedance, low thermal resistance, and high packing density of the power chips. Modules have been designed that can accommodate up to nine power HTP packages.

The cross section of the HTP is illustrated in Figure 2.2.1-1 (not to scale). The silicon chip is die bonded onto the cup-shaped copper package base. Copper foil is thermocompression bonded to the aluminum contacts on the active side of the die. The lid is ceramic with patterned copper direct bonded to the top and bottom surfaces. Copper balls provide feedthrough connections between the top copper and the foil on the active side of the die. The multiple ball contacts and lid seal are joined in a reflow solder operation. The resulting HTP package is hermetic, has a low thermal resistance path to the cooling medium (0.3 °C/W) and has a high standoff voltage (>2500 V).

2.2.2 Advanced Package Concept

The HTP package process can be extended to multiple cavity packages. Figure 2.2.2-1 illustrates this concept with a module containing four MCTs and two diodes as would be required for the 1-MW converter. The package is fabricated on a ceramic substrate using the direct bond process to attach the layers of copper. The characteristics of the module are summarized in Table 2.2.2-1. This concept is not proposed for the 1-MW converter because of the present early stage of HTP development. Furthermore, this module concept does not include components for the snubber and driver circuitry.

Table 2.2.2-1

HTP MCT Module

Devices	Four parallel 200-A, 1000-V MCTs Two parallel 100-A, 1800-V reverse diodes
Dimensions	
Height	~0.75 in
Footprint	1.3125 × 1.3125 in
Weight	75 g
Thermal resistance	
Four MCTs	0.125 °C/W
Two rev. diodes	0.25 °C/W
Snubber circuit	external

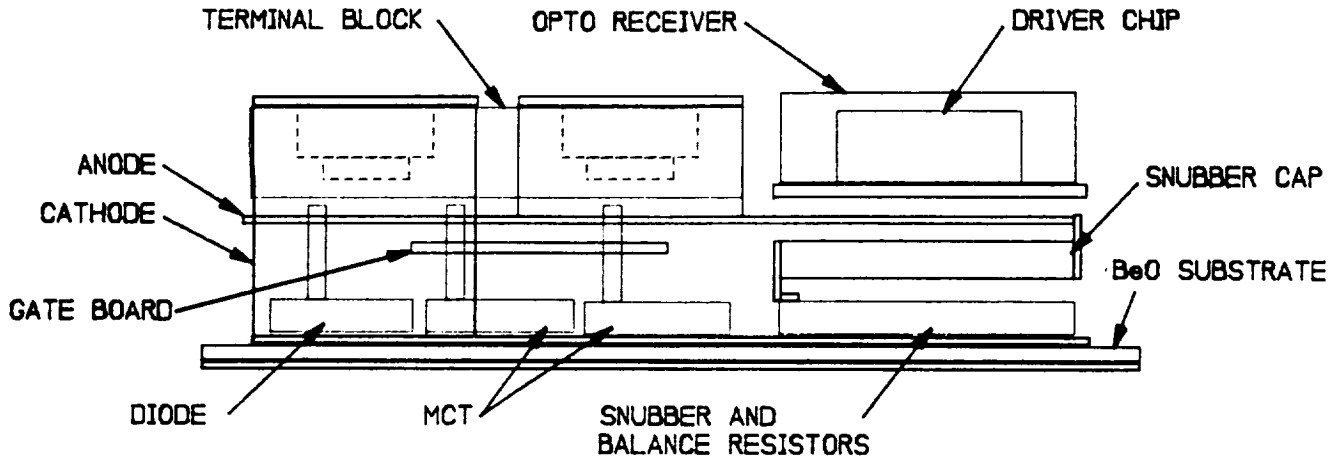

Figure 2.2.3-1. 400-A, 1000-V MCT module; vertical view, 2.6 in × 0.9 in high.

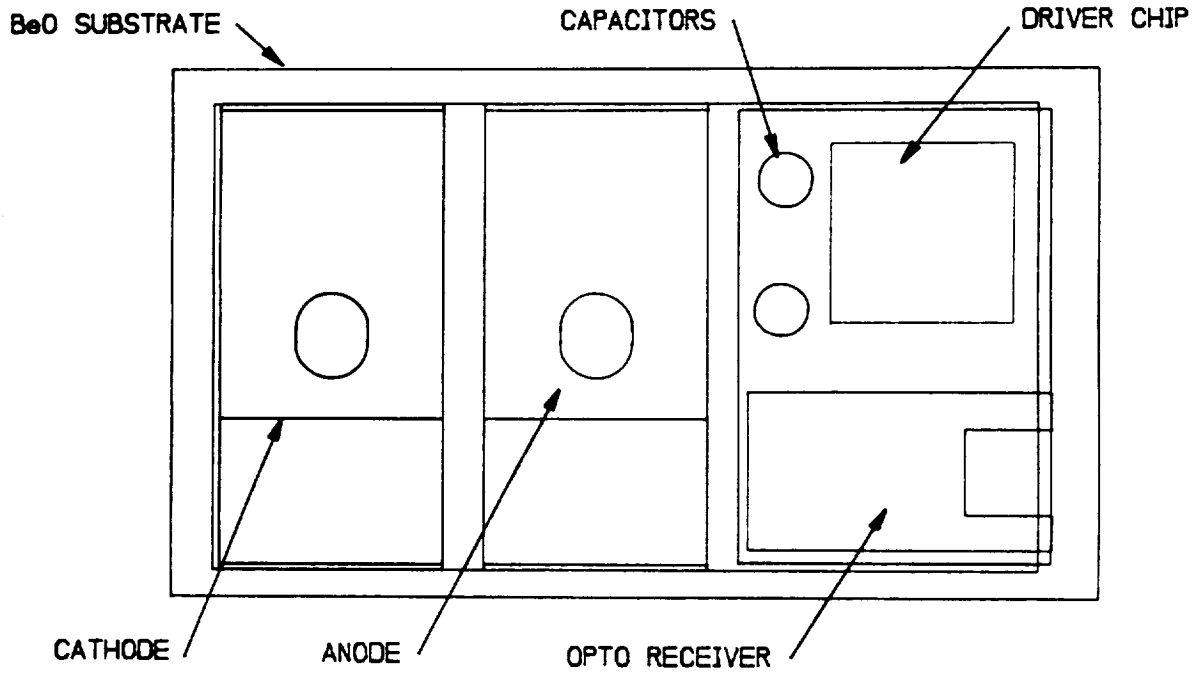

Figure 2.2.3-2. 400-A, 1000-V MCT module; top view, 2.6 in × 1.5 in.

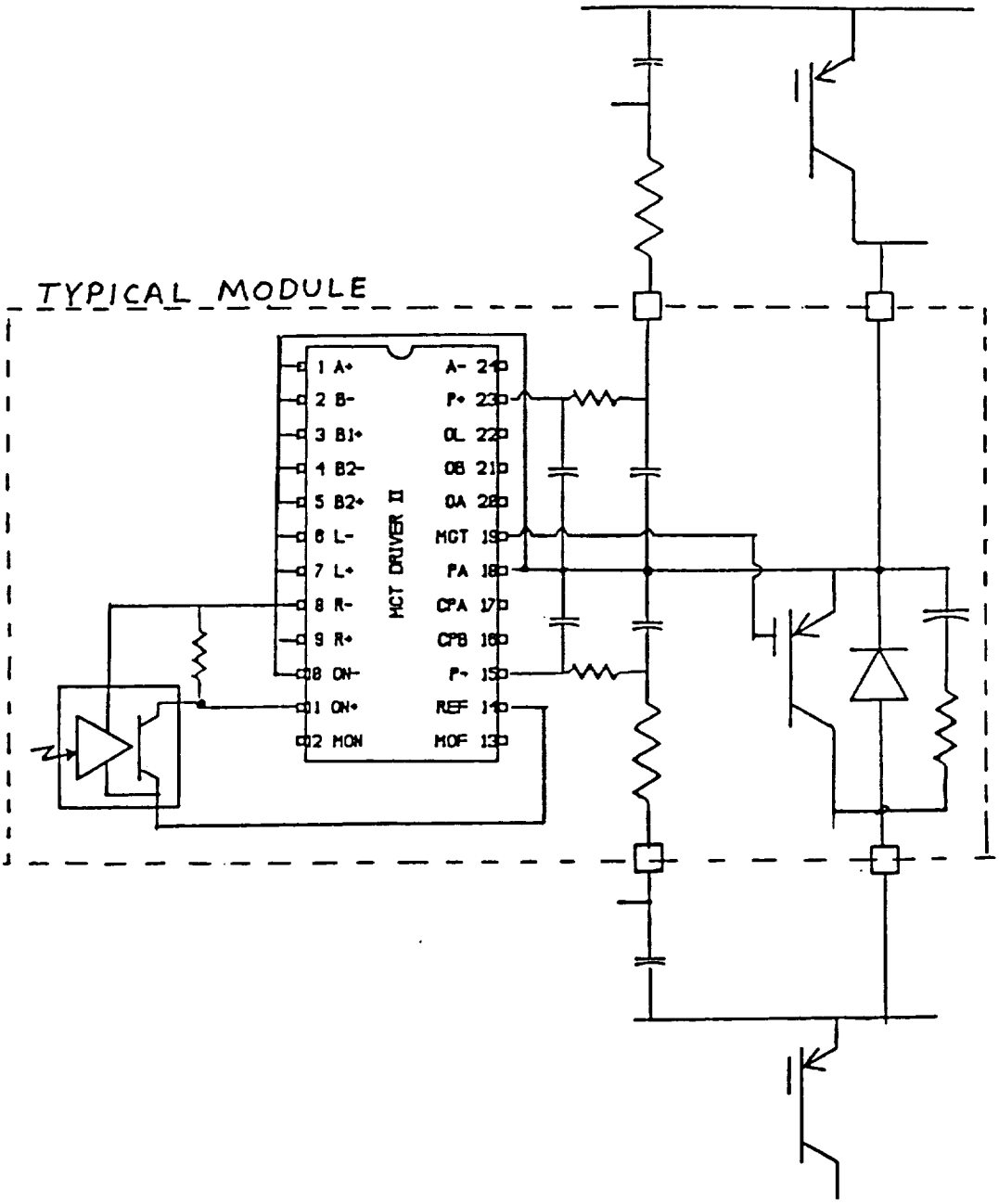

Figure 2.2.3-4. Schematic of MCT module showing method of powering driver circuit.

2.3 MCT MODULE SIMULATION

2.3.1 HSPICE Simulation

The MCT is a functional device comprising a four-layer PNPN bipolar structure, an ON PMOSFET and an OFF NMOSFET. Unfortunately, no commercial simulation program for the PNPN structure is available at the present time. Simple models have been developed in this study with which to expedite the simulation of an MCT having PNP and NPN back-to-back bipolar transistors, the PMOSFET, the NMOSFET and parasitic resistors.

The cross section for a stripe taken through one-half of an MCT is illustrated in Figure 2.3.1-1. A stripe taken outside of the MCT (MCTA) has bipolar transistors, the ON PMOSFET and the OFF NMOSFET. Four inside stripes (MCTBs) have the bipolars and an OFF NMOSFET. Initially, a model having five MCTs in parallel was developed for MCT device simulation. This device model proved to be powerful in providing insight into MCT operation, such as lateral plasma spreading and current sharing between the MCTA and MCTB structures. Next, a "combined" model was developed for fast circuit simulation. Parastic resistor values for these models were extracted from MCT dimensions and doping profiles. Computation time for the circuit model proved to be much faster than that for the device model. Accuracy of the two models was verified by simulations of a dc chopper circuit. The results obtained for each model are very well matched, with the exception of a negligible discrepancy in the very rapid turn-on transient.

For the circuit simulation work, the spread of device parameters typical to production MCTs was accounted for by developing three categories of device types: fast, typical, and slow. The models shown in Figure 2.3.1-1 describe the three catagories in terms of turn-off speed and forward current capability. These models have been used to simulate both typical and worst cases for the MCT in its present application.

The computer platform used for all of the simulation work was the VAX-11/780 located at CRD. The software used was HSPICE. An HSPICE program has been tried and successfully run with a SUN workstation and SABRE software.

2.3.2 Snubber Circuit

A snubber (or balance) circuit equalizes the MCT turn-off voltage sharing required for series operation. Various types of snubbers have been applied to commercial converters. Those circuits provide both transient and steady-state (dc) voltage balancing. Dc voltage balance is accomplished with a resistive divider connected in parallel with each module of a series string of modules. In the present case, a 100-kΩ resistor across each MCT provides adequate balance in compensating for inherent MCT dc leakage current. Transient balancing has been achieved by connecting a series-connected resistor and capacitor in parallel with each MCT module in a series string of modules.

Figure 2.3.2-1 summarizes the snubber simulation results in the worst case for a single "fast" MCT module, series connected to nine "typical" modules, operating in a single-phase dc chopper circuit. Three factors, turn-off time, total loss of the fast module and its snubber, and the reverse voltage, have been evaluated for different snubber resistor and capacitor values. Reviewing the results, the combination of a 7.5-Ω resistor and a 0.06-μF capacitor provides the best performance compromise among the variables of power loss, voltage overshoot, and turn-off fall-time. The optimized snubber was used in the H-bridge converter simulation work conducted in HSPICE.

One FAST MCT module in series with 9 TYPI modules, single phase chopper (5 kV, 200 A, 23.80 kHz)

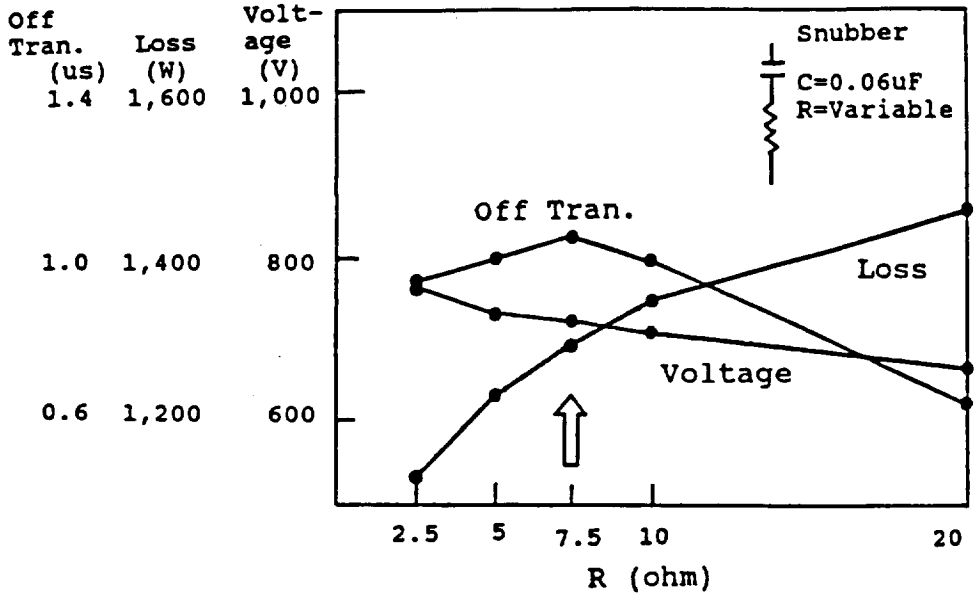

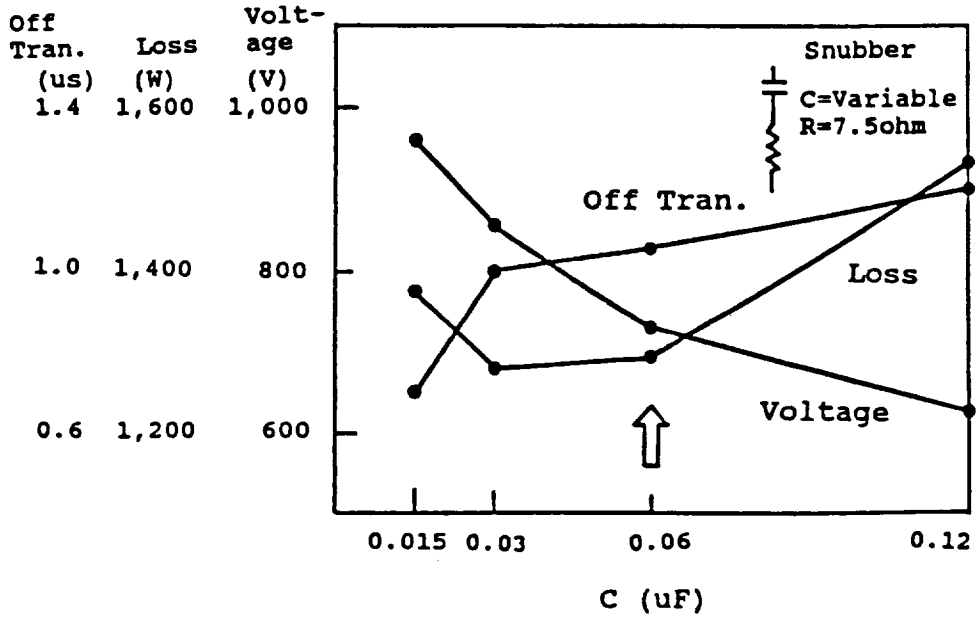

Figure 2.3.2-1. Snubber simulation.

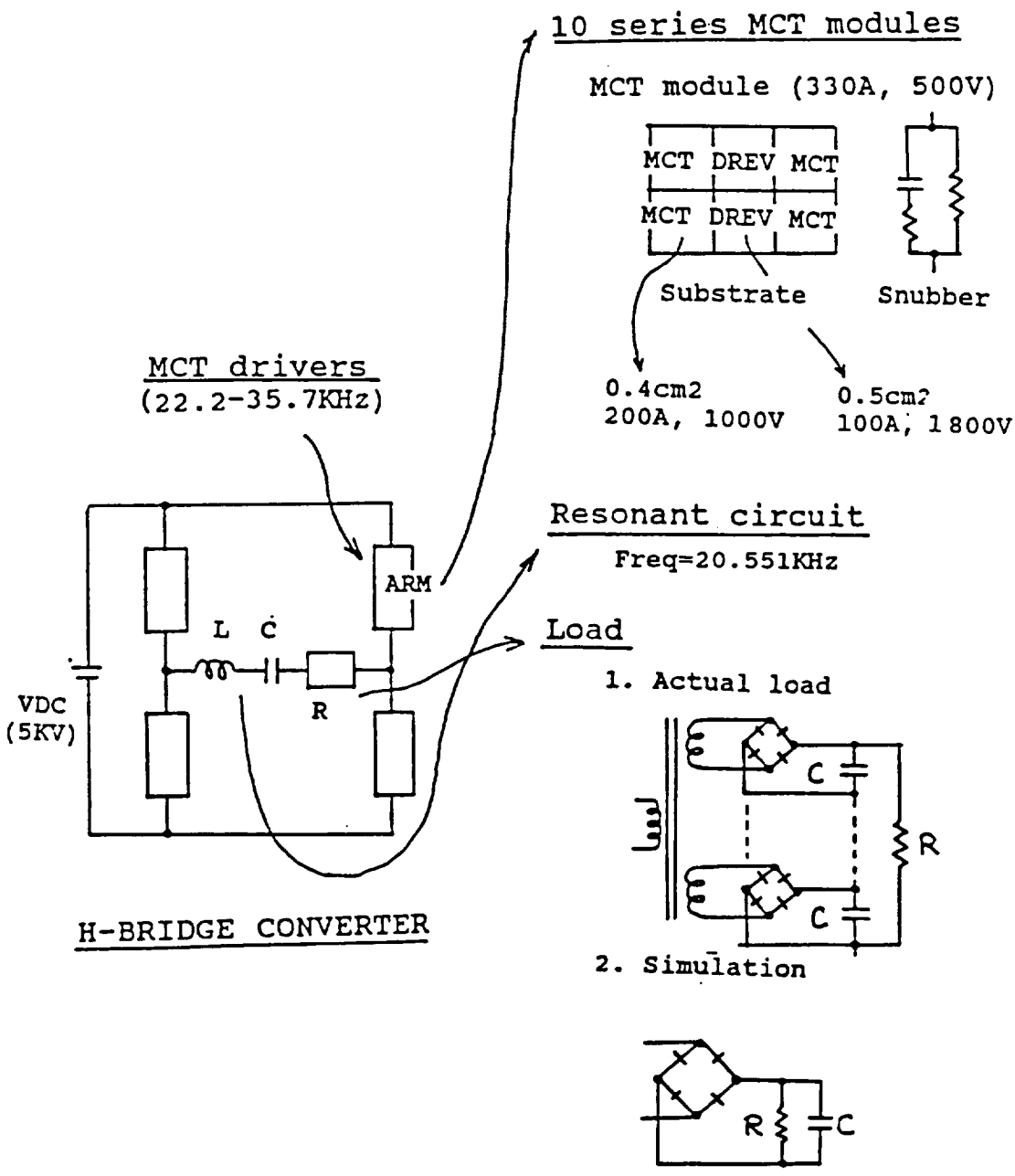

Figure 2.3.4-1. NASA 5-kV, 1-MW H-bridge converter.

Table 2.3.4-1

1-MW H-Bridge Converter

Cycle time (μs)	45.0	42.0	37.0	28.0
Frequency (kHz)	22.222	23.80	27.03	35.71
Load resistor (Ω)	19.926	41.377	84.645	190.50
Load output (kW)	1031.4	498.6	238.4	108.6
Total loss (kW)	42.4	31.4	27.7	31.2
Power efficiency (%)	96.1	94.1	89.6	77.7
Common parameters				
Dc voltage	5000 V			
Filter capacitor	38.7 μF			
Resonant inductor	300 μH			
Resonant capacitor	0.200 μF			
Resonant frequency	20.551 kHz			
Load dc voltage	4546 V			

Note: All modules consist of "typical" MCTs

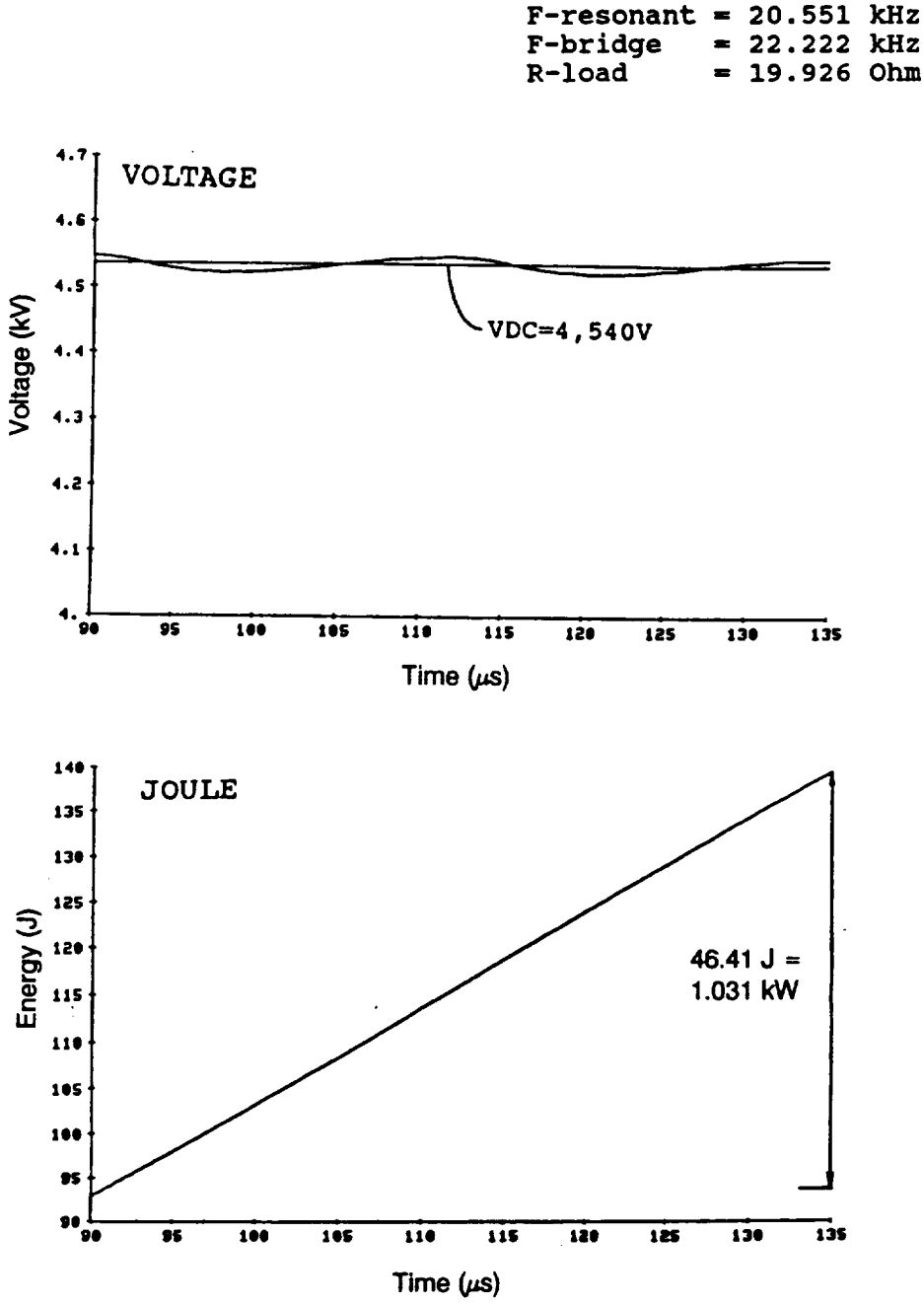

Figure 2.3.4-3. 1-MW H-bridge converter – output simulation.

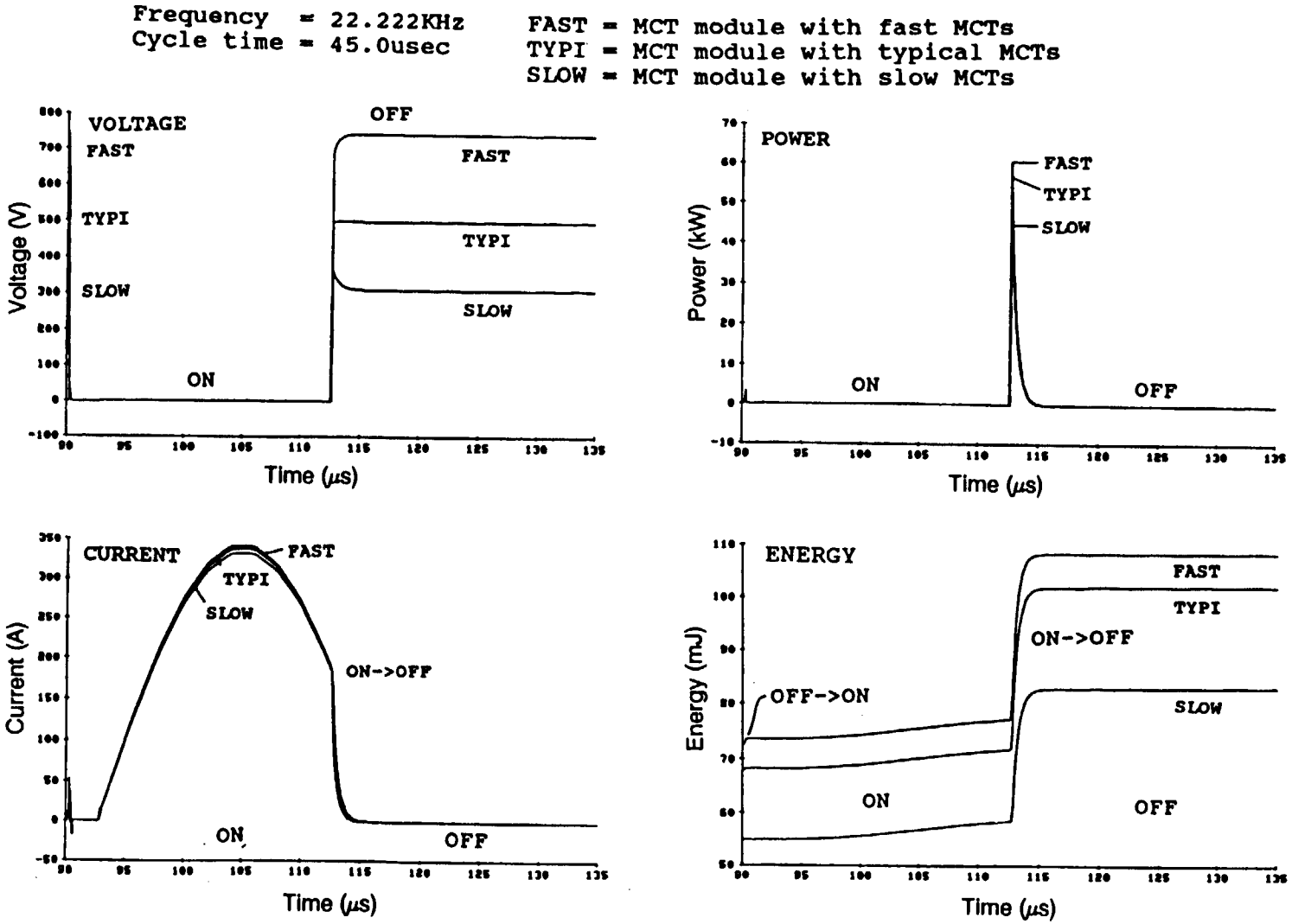

Figure 2.3.5-2. MCT device simulation.

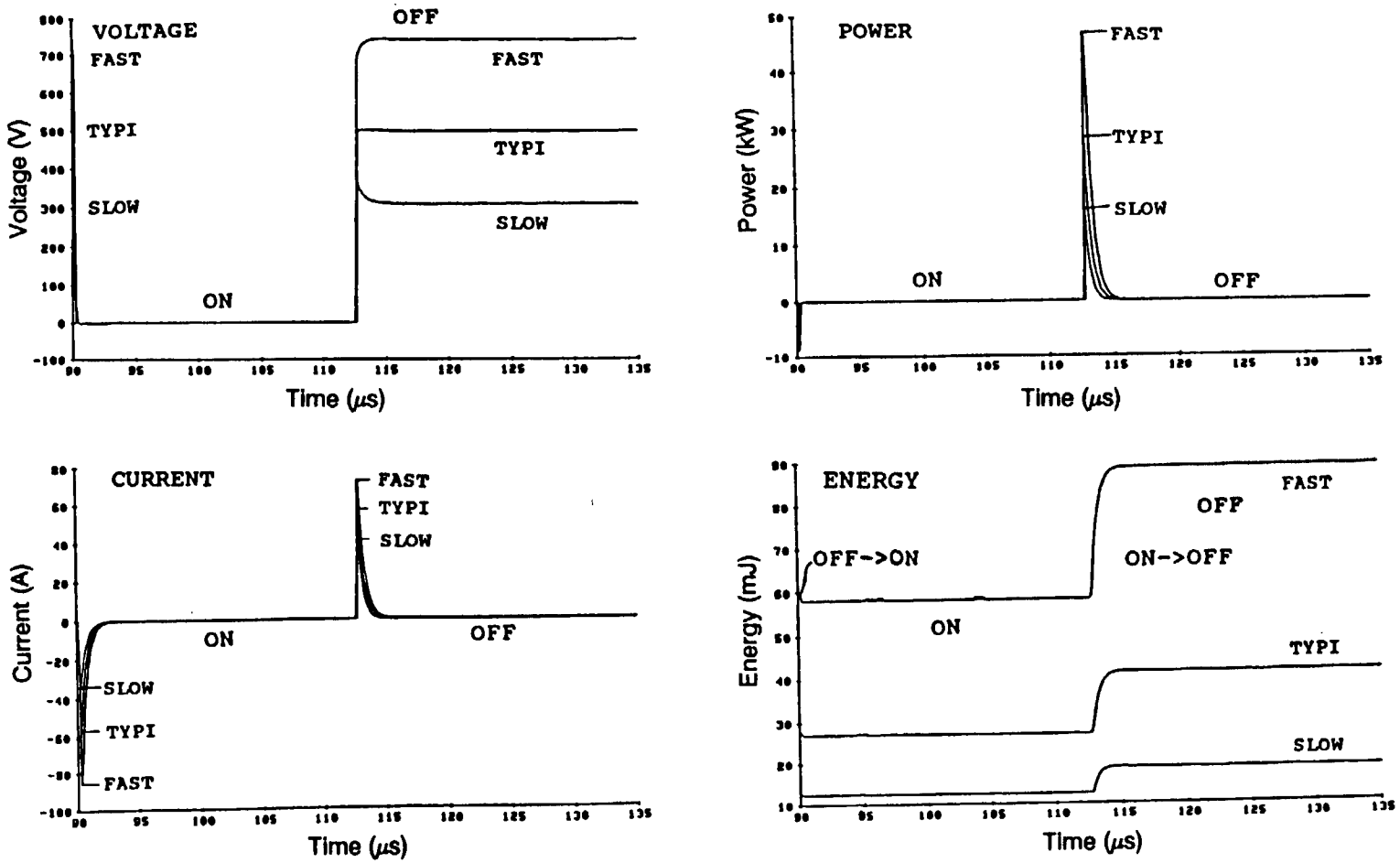

Figure 2.3.5-4. Snubber circuit simulation.

Table 2.3.5-3 tabulates loss for the MCT modules at different frequencies. The MCT device loss decreases at higher frequencies because output power and therefore device peak current is decreasing. Snubber loss increases with frequency and is therefore a maximum at 35.71 kHz. The net result of these competing loss mechanisms is a decrease in total loss to 27.03 kHz followed by an increase at 37.71 kHz.

The worst-case loss for the MCT module is 1440 W for a fast module, occurring at 22.22 kHz. For the system worst case, the data for the typical case applies. As an example, the 1060 W for a typical module loss multiplied by 40 modules yields 42.22 kW at 22.22 kHz, which yields 42.22 kW of loss for the system worst case.

Power loss for each type of MCT device is summarized in Tables 2.3.5-4 through 2.3.5-6. MCT device power loss decreases with increasing frequency from 22.22 to 35.71 kHz (Table 2.3.5-4) with the greatest power loss being exhibited by all three MCT types at 22.22 kHz.

The reverse diodes show less dependency on module types because they are active only during the ON transient. As shown in Table 2.3.5-5, forward current decreases very rapidly at higher frequency. Loss is always negligibly small.

The snubber circuit losses in Table 2.3.5-6 can be summarized as follows: Loss in the R-C snubber is a function of reverse voltage and frequency. Snubber loss for the typical module is proportional to frequency, because the reverse voltage is constant at 500 V. Snubber loss for the fast module is roughly constant, because the reverse voltage decreases at higher frequency. Snubber loss for the slow module increases very rapidly with increasing frequency because the reverse voltage increases with frequency. Snubber loss in the worst case occurs with the fast module at 35.71 kHz.

2.3.6 Losses and Temperature Rise

Table 2.3.6-1 tabulates the losses for the MCT module, MCT device, reverse diode, and snubber for the typical and worst case. The heat generated by these losses is to be removed by the cooling system. The substrate temperature is assumed to be 0 °C. The thermal resistances for the MCT and reverse diode are 0.125 and 0.25 °C/W, respectively. Temperature rise from the heat sink to the MCT junction is 100 °C in the worst case.

2.4 MCT Inverter Hardware

A sketch of the proposed MCT inverter hardware is shown in Figure 2.4-1. The inverter hardware structure comprises 40 MCT modules mounted on a heat sink and interconnected electrically by a power bus structure (not shown). The 12×17-in mounting surface area is dictated by the 1.5×2.5-in module footprint, assuming 0.1 in intermodule spacing and some edge margin. The heat sink is shown as a finned structure to support convection hydrogen cooling. The total volume is 0.354 ft^3 and the mass is estimated at 7 kg exclusive of the power bus electrical system. The mass of the bus system is estimated to be 1 kg, which yields a total mass of 8 kg for the inverter hardware.

Table 2.3.5-4

MCT Device

Cycle time (μs)	45.0	42.0	37.0	28.0
Frequency (kHz)	22.222	23.80	27.03	35.71
Fast MCT				
Max rev voltage (V)	743	676	623	577
Max fwd current				
-ON transient (A)	37	73	89	77
-ON cycle (A)	342	159	75	32
Power loss (W)	796	430	285	224
Typical MCT				
Max rev voltage (V)	499	499	499	499
Max fwd current				
-ON transient (A)	54	87	105	116
-ON cycle (A)	339	159	76	35
Power loss (W)	796	430	285	224
Slow MCT				
Max rev voltage (V)	311	354	394	425
Max fwd current				
-ON transient (A)	16	65	92	113
-ON cycle (A)	333	157	75	31
Power loss (W)	624	428	338	305

Table 2.3.5-6

Snubber Circuit

Cycle time (μs)	45.0	42.0	37.0	28.0
Frequency (kHz)	22.222	23.80	27.03	35.71
BAL of fast module				
Max rev voltage (V)	743	676	623	577
Peak current				
-Negative (A)	-86	-83	-76	-70
-Positive (A)	72	72	68	60
Power loss (W)	639	580	566	651
BAL of typical module				
Max rev voltage (V)	499	499	499	499
Peak current				
-Negative (A)	-57	-58	-59	-59
-Positive (A)	56	58	59	60
Power loss (W)	279	329	378	507
BAL of slow module				
Max rev voltage (V)	311	354	394	425
Peak current				
-Negative (A)	-34	-40	-46	-49
-Positive (A)	44	49	53	54
Power loss (W)	136	184	254	386

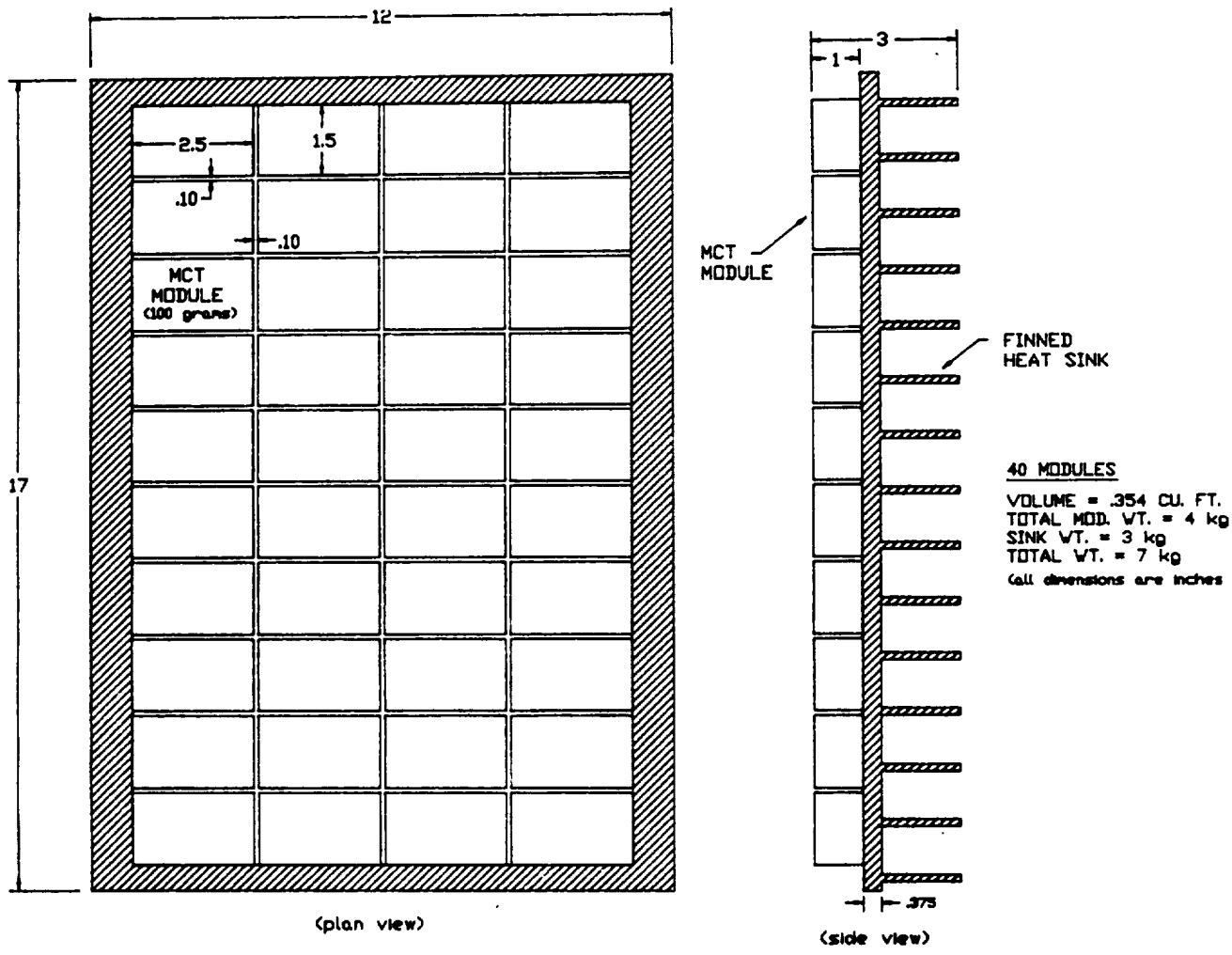

Figure 2.4-1. Proposed MCT inverter hardware.

Section 3

TRANSFORMER-LINKED DC-TO-DC CONVERTER SYSTEM

3.1 Converter System Topology

The dc-to-dc converter system that GE-CRD is developing includes an inverter-rectifier cascade with an ac transformer link. A block diagram of the system topology is shown in Figure 3.1-1. The first block after the dc input circuit breaker or other fault protection device is a dc filter, which provides a low impedance source of voltage for the inverter. The second block is a dc-to-ac full-bridge (H-bridge) inverter, which is generally preferred for high-power equipment so that the power semiconductors can be switched with a phase displacement to develop a controllable ac voltage waveform. A switching frequency of 20 kHz or higher is required to optimize the size of the magnetic and capacitive components.

The third block is a step-up transformer which produces a high voltage ac waveform. The next block is an ac-to-dc rectifier, composed of either high-voltage strings of diodes fed from a single secondary winding or, as in the present case, multiple lower voltage windings each with its own rectifier, which are in turn connected in series. The final block is a multiple-section dc filter capacitor, which reduces the ripple voltage on the output to specified levels.

This approach, using simple diode rectifiers, avoids the need for controlled high-side switches, but places all the duty of regulation on the low-side switches, which must be controlled devices to obtain dc-to-ac inversion, in any case. The control circuit senses, at a minimum, the output voltage and feeds it back to the control circuit for the low-side switches. The control circuit modulates the dc-to-ac inverter pulse-width and/or frequency, which adjusts the output voltage to the desired level.

3.1.1 Super-Resonant Inverter

The series super-resonant inverter topology has been developed at GE for several applications [1-5]. This power conversion technique overcomes some of the disadvantages of conventional PWM switchmode conversion as frequency is increased, such as higher switching losses in the power semiconductors and increased EMI caused by the square-wave nature of the current waveform. Resonant mode operation results in a near sinusoidal current waveform in the power switches, in the resonant load elements, and in the transformer windings, which reduces the potential for electromagnetic emissions. Super-resonant operation (operation above the resonant frequency of the tank) employing gate turn-off devices provides a number of additional advantages:

- Lossless capacitive snubbers can be used for switch protection at turn-off.
- Since the power switch turns on while its anti-parallel diode is conducting, the switching loss during turn-on is very low.
- Medium-speed inverter diodes can be used, rather than more costly high-speed diodes, again because power switch turn-on occurs while the diode is conducting.
- No di/dt limiting or snubber inductors are needed.
- Operation above the resonant frequency of the L-C tank permits voltage control through variable frequency, while maintaining a minimum weight transformer.

- The parasitic leakage inductance of a high-voltage transformer can be utilized as part of the resonant load.
- The current-source nature of the resonant inverter provides a safety margin under load fault conditions and permits the paralleling of power stages for increased rating.

Control of the output voltage is achieved through a combination of frequency modulation [6] and phase modulation. The operating frequency will be in the range 20 to 50 kHz. Transformer winding capacitance, magnetizing inductance, and leakage inductance are second-order effects that modify the ideal series-resonant behavior of the converter circuit. In particular, the effect of winding capacitance is quite critical, and a transformer design to minimize the effective ac capacitance is necessary.

Theory of Operation

The inverter power stage (Figure 3.1.1-1) is a full-wave bridge using MCTs with anti-parallel fast diodes for the power switch. Snubber capacitors are placed across each power switch. Operating in a nearly lossless manner under FM control, the snubbers are used chiefly to limit dv/dt for EMI suppression and to assist the anti-parallel diodes in limiting voltage overshoot at the close of a conduction cycle caused by diode turn-on time. The dc bus capacitor bank must carry the ac component of the input current while maintaining very low ripple at the operating frequency. The gate drivers provide positive voltage for MCT turn-on and conduction and a negative voltage for turn-off and maintenance of the off state. The inverter output voltage (V_{AB}) is applied directly to the primary winding of the high-voltage transformer in series with the resonant tank.

For simplifying the following discussion of inverter conduction modes, (Figure 3.1.1-2), the high-voltage transformer, its output rectifier, the filter capacitors, and the load have been replaced by a voltage source (the charged output capacitor) inserted in a full-wave bridge rectifier. The conduction sequence during one cycle of operation in FM control mode for super-resonant operation (where the series resonant load behaves inductively) is shown in Figure 3.1.1-2, where the heavy lines indicate those components that are conducting current. Simultaneous conduction of Q1 and Q4 has resulted in the resonant increase in current in the arrow direction of Figure 3.1.1-2a. Simultaneous turn-off of Q1 and Q2 results in the rapid fall of the node A voltage (rise of node B voltage), because the load current is transitioned to the node capacitance (snubber capacitance plus device and stray capacitances). The tank current remains essentially constant during the relatively short transition time due to the action of the resonant inductor. Node B voltage falls (node A voltage rises) until the anti-parallel diodes D2 and D3 conduct, clamping the node voltages to a diode drop relative to the rail voltages.

In the conduction mode (diode conduction) that results (Figure 3.1.1-2b), the current decreases to zero. Early in the diode conduction interval, Q2 and Q3 are switched on, after a short "lockout" interval to prevent potentially disastrous "shoot-through" or simultaneous conduction of Q1 and Q2 or Q3 and Q4. The current now reverses, increasing in magnitude resonantly via the switches Q2 and Q3 (Figure 3.1.1-2c). Simultaneous turn-off of the power switches Q3 and Q2 is commanded by the control circuit (at a time in the conduction cycle, which is determined by the required average current), resulting in the rapid fall of the node B voltage (rise of node A voltage) caused by the transition of load current to the node capacitance, as discussed earlier. Pickup of the current by the anti-parallel diodes D1 and D4 results in the conduction mode of Figure 3.1.1-2d. After the lockout interval, switches Q1 and Q2 are turned on and the conduction mode of Figure 3.1.1-2a results, completing the inverter conduction cycle.

The full H-bridge configuration is more suitable for high-power equipment and also allows operation with a phase shift between switching of the two legs. This applies a quasi-square wave of voltage to the resonant circuit, and affords another method of voltage control, in addition to frequency adjustment. The flexibility of the circuit is much improved, and it may be operated over a wider range of load at nearly constant frequency, which is desirable in most applications.

In summary, a super-resonant converter needs only shunt capacitor snubbers, which are quite small with high-speed turn-off devices and, in any case, operate in a lossless mode. The devices turn on as the resonant current crosses from an anti-parallel diode at near-zero voltage, so turn-on loss is practically eliminated. The smoother current switching reduces EMI. Resonant converters can be designed for self-protection by limiting overloads, a necessary feature in high-voltage systems where random voltage breakdown is almost unavoidable [7].

Three-Phase Circuit Option

At conventional power frequencies, practically all high-power equipment is configured in a 3-phase circuit arrangement. At some power level the reduced total rating of a 3-phase circuit overcomes the disadvantage of division into three parts. At 60 Hz, a 1-MW converter would certainly be a 3-phase circuit. A 3-phase version of the present series super-resonant converter is shown in Figure 3.1.1-3. Operating at 20 kHz, this arrangement will become lighter than the single-phase circuit at some power level. This power level may be above or below 1 MW; to our knowledge, no tradeoff study has been done. It may be worthwhile to conduct such a study at the start of Phase 2.

In Figure 3.1.1-3, three single-phase H-bridges are operated with a mutual 120-degree phase displacement. Each bridge generates an adjustable quasi-square wave for voltage control, which is applied to an individual series-resonant L-C tank circuit in series with a primary winding of the main transformer. The main transformer is wound on a 3-phase E-core. A small auxiliary transformer (about 3% of the main transformer in size) has three coupled windings (one in each phase) that absorb the zero-sequence voltages (third harmonic and its multiples), eliminating these components from the rest of the circuit. This allows a significant reduction in the rating of the main transformer and of the resonant inductors.

The high-voltage secondary windings are connected in delta to a 3-phase bridge diode rectifier and filter capacitor. As in the single-phase case, there are N sections corresponding to the N layers of the secondary windings, which are connected in series on the dc side. The ripple at both input and output is 6-pulse ($6 * 20$ kHz = 120 kHz) instead of 2-pulse ($2 * 20$ kHz = 40 kHz), which greatly reduces the size of the filter capacitors. While the total rating of the components is reduced, the H-bridges, the series capacitance and inductance, and the transformer coils are divided into three parts, which may increase their physical size.

3.1.2 Prime Power Interaction

The behavior of the prime power source, assumed to be an array of fuel cells, is a critical factor in the design of the power converter. In a specific system, the steady-state (dc) voltage-current characteristics under best- and worst-case extreme conditions are required for establishing the range of input variables that the converter must accommodate. The series super-resonant power converter circuit, with suitable design, will be able to operate from a variable source having the characteristics of typical fuel cells. However, for the present preliminary study, NASA has requested that an ideal source at fixed voltage be assumed, so that size and weight estimates will approach the best attainable. For a number of reasons, it appears that an input voltage of 5000 V will be near optimum for achieving minimum size, so

this value will be assumed for the present study. Then, for 1 MW, the average dc current will be 200 A, neglecting losses.

The maximum ac ripple current that the power source can tolerate, or the maximum ripple voltage that the converter can tolerate, will determine the design of the input filter. Because no requirements have been specified, a typical condition has been assumed for the present study. The rms ac ripple current from the power source to the converter at full load is about 100 A. Assuming that a maximum rms ripple voltage of 10% (500 V) is allowable, then the source impedance must be limited to 5 Ω at the ripple frequency of 40 kHz. The input filter capacitance having this reactance is 0.8 μF.

3.1.3 Load Range Interaction

A second critical factor for the design of the power converter is the characteristics of the load. In particular, the range of load current is needed for establishing the range of output variables that the converter must accommodate. This is important for the design and stabilization of the control system. Also, the maximum ac ripple voltage and current that the load can tolerate will determine the design of the output filter. For the present design, the output filter capacitance C_d = 80 nF has been selected to reduce the output ripple voltage (at 40 kHz) to less than 0.25% rms. This will store 400 J at 100 kV, requiring a crowbar for protection of the load.

3.1.4 Cooling Systems

Efficient removal of heat from the converter system can have a significant impact upon weight and size. With the option of cryogenic cooling using liquid hydrogen, it is feasible to maintain a cold plate at any desired temperature above 21 K. The cooling system design then reduces to selecting an optimum operating temperature and achieving a reasonable thermal gradient from the hot spots to the cold plate. Alternatively, as in our present concept for cooling at least the transformer, a similar system employing hydrogen gas circulation to maintain an optimum operating temperature can be used.

NASA has indicated that a reasonable assumption for the duty cycle of typical loads that can be fed by the converter is 1000 s operation at full load in an orbital period of 90 min, or 18.5%. This will be helpful in the thermal design of the transformer, but the semiconductor switches will have a much shorter time thermal constant, and will be subject to effectively continuous duty.

3.2 High-Voltage Transformer Design

Of the total weight objective of 100 kg for a 1-MW converter, about 35 kg can be allocated to the transformer. The design frequency for the transformer will be the minimum operating frequency of 20 kHz, since at higher frequencies the flux level will be reduced, such that the core loss will be lower. For operating bursts of 1000 s with intervals for cooling, the relatively long thermal time constant of the magnetic structure will allow higher losses than for a converter in continuous operation.

A special high-voltage transformer-rectifier design is needed to minimize reflected capacitance at the primary side of the transformer. In the proposed core-type structure (Figure 3.2-1), two coils are employed, one on each leg of the core. The primary windings are connected in parallel. This arrangement has lower weight than a shell-type structure, with a single coil on one leg of the core, or on the center leg of an E-core. The secondary windings are divided into sections, each feeding a section of the rectifier. By making series connections of these sections on the dc side (Figure 3.2-2), the effective ac capacitance reflected to the pri-

mary side can be reduced to the low value required for proper operation and simple control of the series super-resonant inverter. In Figure 3.2-2, each section of the secondary winding is a single layer, and all the dc capacitors are equal in value.

3.2.1 Interconnection of Coils

A possible problem with this approach is the effect of differential leakage reactance between layers of the secondary winding on the voltage distribution along the series string of rectifiers and dc filter capacitors. It is expected that the voltage will be higher on the first level next to the primary winding than on the last layer. The voltage drop caused by leakage reactance is proportional to load and frequency (ωLI), and the relative effect (% unbalance) is determined by the factor ($\omega LI/V$). Obviously, this is an undesirable situation for the rectifiers and capacitors.

The unbalance might be compensated by winding more turns on the outer layers, but this is undesirable for coil construction. A coil design having a relatively long winding traverse and a small build should minimize the unbalance between leakage inductances, and may reduce the voltage difference between levels to where it is not a significant problem. For a coil of different proportions, particularly a relatively short winding traverse and a large build, the voltage distribution should be considered carefully.

The effects of voltage unbalance and a possible method of compensation are illustrated for three alternative interconnections of the two coils to the rectifiers in Figures 3.2-2, 3.2.1-1, and 3.2.1-2. While a half-bridge rectifier is shown in these figures, a full-bridge could also be used in each case.

In Figure 3.2-2, the coils are not interconnected; one coil produces +50 kV dc output, and the other −50 kV dc. It is assumed that the center of the dc output is grounded, so that the insulation must withstand only ±50 kV to ground, instead of 100 kV. This minimizes the insulation thickness and thermal resistance. With a center ground next to the first layers, the insulation to the primary windings and core is minimized. Insulation for 50 kV dc is needed over the outer layers of each coil, for 100 kV between the coils. With symmetrical coils, the ±50 kV dc outputs should be balanced with respect to ground. However, there can be unbalance between the voltage levels along the series string on each side.

If the load requires 100 kV dc to ground, as expected, then the extra insulation required will result in a slightly larger size. In this case, the interconnection shown in Figure 3.2.1-1 is better. Corresponding layers of the two coils are connected in series, which halves the number of diodes and capacitors required, although the total rating is the same as for Figure 3.2-2. Again, with ground next to the first layers, the insulation to the primary windings and core is minimized. Also, with the outer layers of both coils at 100 kV, the insulation between coils is minimized. However, some unbalance will again occur between the voltage levels along the series string on each coil.

In Figure 3.2.1-2, opposite layers of the two coils are connected in series; the first layer on one side is connected to the last layer on the other side, and so on. This should improve the balance between the voltage levels along the series string. However, the insulation requirements of the two coils are asymmetrical. While the first layer of the left coil is near ground, the first layer of the right coil is near 100 kV. Conversely, the last layer of the left coil is near 100 kV and the last layer of the right coil is near ground. For this reason, the interconnection of Figure 3.2.1-1 is much preferred and will be used unless unbalance between the voltage levels is found to be a serious problem.

3.2.2 Coil Design

The coil design for a high-frequency, high-voltage, high-power transformer is particularly difficult if light weight is desired. Conventional commercial designs of high-voltage coils rely on paper and oil or air as the major insulation to ground. Using a conservative value of the voltage gradient allowed across such insulation, which occupies much more window space than the copper because of wide spacing from coil to ground, it is found that a large, heavy core is required. The overall size of the transformer is greatly affected by the voltage rating, and the variation with current (power) rating is relatively small.

It was concluded from earlier studies that any transformer design using oil (or other fluid) alone as the major insulation to ground cannot meet the size goals. Tight enclosure of at least the secondary windings in some material allowing significantly higher voltage gradient stresses seems to be the solution. The use of interlayer insulation that permits higher voltage gradients is also indicated. However, such high-gradient insulating materials have higher dielectric permittivity than oil, gas or paper. Because the spacing is closer and the dielectric permittivity is higher, an increase in capacitance results from both factors. The resolution of this difficulty is to divide the secondary windings into sections, each feeding a section of the rectifier, as previously discussed.

To implement this construction technique, the design and manufacture of the high-gradient coil forms is critical. Integration of each layer of the secondary winding with a section of the rectifier and filter capacitor is necessary to minimize the insulation space and the ac winding capacitance. The high-voltage secondary windings will be completely enclosed within precision-molded solid insulation forms of a material such as polypropylene, for which a design gradient of 800 kV/cm (2 kV/mil) is assumed. Sections of the coil forms must fit together very tightly (0.1 mm press fit), so that the high-gradient electric field is contained within the assembly and the high dielectric strength of polypropylene allows close spacing to the core and nearby grounded structures.

In making forms of this type, proper allowances must be made for shrinkage and other factors; size and shape limitations could restrict the options of transformer geometry. A filler material such as talcum powder may be used to increase the thermal conductivity. The cost of making the molds for the forms is expected to be high, so the design should be firm before manufacture. Therefore, it is proposed that the coil forms be fabricated by other methods during this development program, postponing the use of molds until any future production is undertaken.

Our original concept was to enclose the rectifier diodes and dc filter capacitors with the secondary windings in extended forms of polypropylene insulation, distributing the diodes and capacitors around the periphery of the coil. In this way, all the high-voltage interconnections except the output lead are contained within the high-gradient insulation system. This type of construction has been used in a commercial application at a lower power level and low duty cycle, where thermal problems are not acute. However, because of the disparity in the heat generation and temperature limits of the transformer coils, the rectifier diodes, and the capacitors, this concept has been modified. We now propose to group the diodes and capacitors at one end of the transformer, perhaps with a polypropylene conduit for the many leads. This arrangement allows the outer surface of the coils to be in direct contact with the cooling medium.

Round Litz

TYPE 1

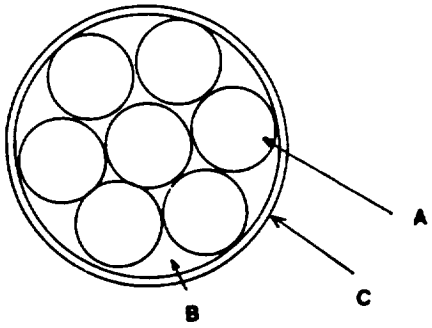

A. Insulated wire.

B. Several twisted wires.

C. Outer insulation of textile yarn (optional).

TYPE 2

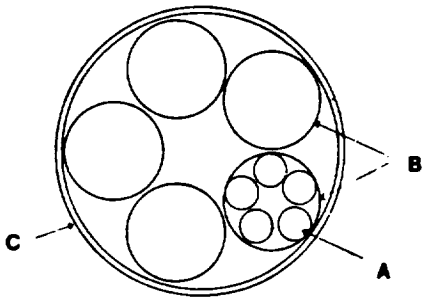

A. Insulated wire.

B. Twisted wires, without textile insulation.

C. Outer insulation over component groups of twisted wires (optional).

Rectangular Braided Litz

TYPE 7

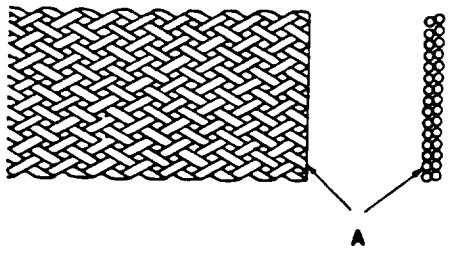

A. One wire or a group of insulated wires.

Rectangular Compacted Litz *

TYPE 8

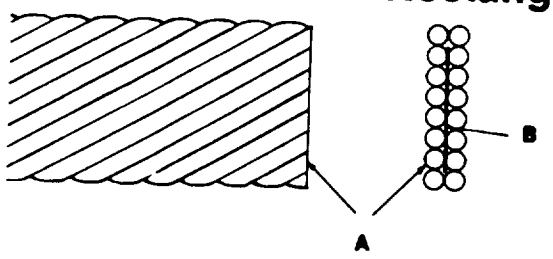

A. One wire or a group of insulated wires.

B. Insulating strip.

* New England U. S. Patent 4439256

Figure 3.2.2-1. Types of litz conductor.

3.2.4 Packaging and Cooling

The thermal and packaging design of the high-voltage transformer-rectifier is a critical problem in minimizing weight. In our original concept, the rectifier diodes and dc filter capacitors were to be enclosed with the secondary windings in extended forms of polypropylene insulation, distributing the diodes and capacitors around the periphery of the coil. This assembly was to be enclosed together with the resonant inductor in an aluminum tank filled with oil for insulation and cooling. The dielectric liquid (isopropylbiphenyl) proposed by Maxwell Laboratories for impregnating the capacitors can also be used for the transformer and inductor. A very much simplified initial analysis of the thermal behavior of the system indicated that cooling will be difficult. The thermal dissipation at the surfaces of the core and coils is high, and forced fluid cooling in addition to conduction is necessary.

In the presence of high-frequency magnetic fields, metal tubing for the cooling fluid is undesirable, as are metal sinks for conducting heat. Therefore, forced convection of the liquid insulating oil, in direct contact with the transformer structure, was proposed. The oil would be cooled in a liquid hydrogen heat exchanger. With the high-voltage windings surrounded by the rectifier and filter capacitors enclosed in solid insulation, rendering the oil inside stagnant, conduction of heat through this structure to the outer surface was a severe limiting factor. The poor thermal conductivity of the insulating material and the desired temperature limit of 60 °C for the polypropylene filter capacitors are particularly limiting, especially in view of the added losses of the rectifier diodes.

Because of the disparity in the heat generation and temperature limits of the transformer coils, the rectifier diodes, and the filter capacitors, our original concept for enclosing these components with the secondary windings in solid polypropylene insulation was modified. We now propose to group the diodes and capacitors at one end of the transformer, perhaps with an insulating conduit for the many leads. This arrangement allows the outer surface of the coils to be in direct contact with the cooling medium. All these components and the resonant inductor are still expected to be contained within the transformer tank. Detailed work on heat transfer in this arrangement has confirmed that forced oil cooling will be effective. Because many of the heat transfer formulas are quite complex, computer routines were written to speed the calculations and to allow tradeoff options to be studied in depth.

However, to eliminate the weight of an oil to liquid hydrogen heat exchanger, the idea of employing direct gaseous hydrogen cooling is now proposed, as in the scheme conceived by Maxwell Laboratories for their converter system. This should also allow the metal tank to be replaced by a lightweight enclosure, including the inverter and all other components as well. Estimates of heat transfer coefficients obtainable with gaseous hydrogen cooling show that it is feasible and should save considerable weight, but the effect on the dielectric insulation system will need further study in Phase 2. The heat transfer coefficient is less than for comparable oil cooling, leading to a higher but not critical temperature rise.

Thermal Conduction

Small size leads to high losses per unit volume, resulting in large thermal gradients and a significant rise within the core and coils of the hot-spot temperature above the surface temperature. Literature on the difficult problem of calculating the hot-spot temperature was consulted. A relatively simple method of analyzing the thermal behavior of the system was developed, leading to a formula for estimating the temperature rise of cores and coils with anisotropic thermal properties. This should be sufficiently accurate for engineering design purposes, at least in the present Phase 1 of this project. In later phases, it may be desirable to

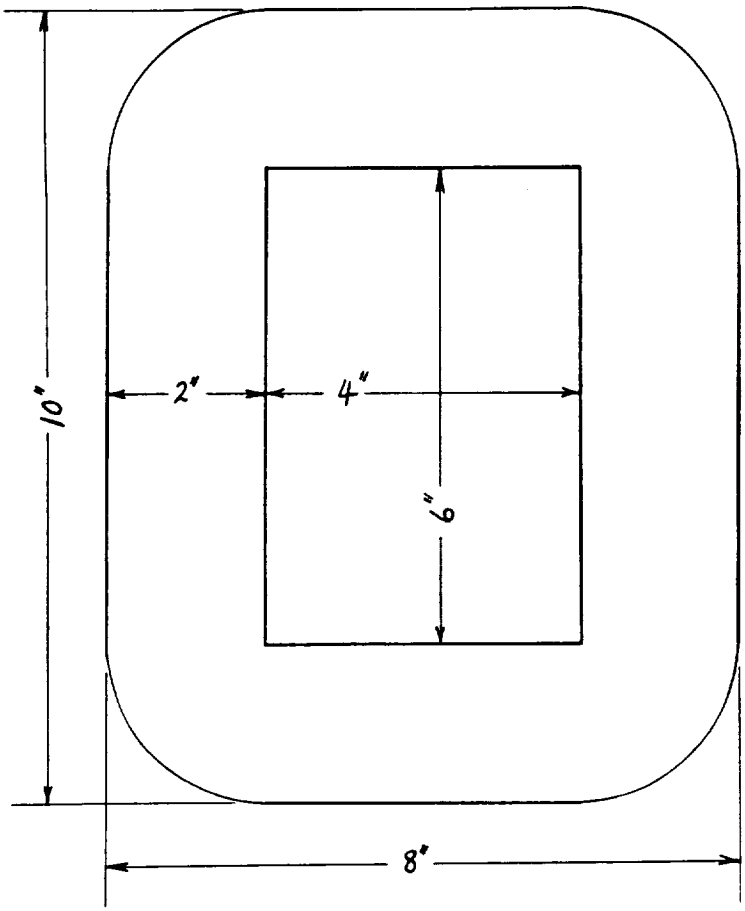

Figure 3.2.5-1. Transformer core dimensions.

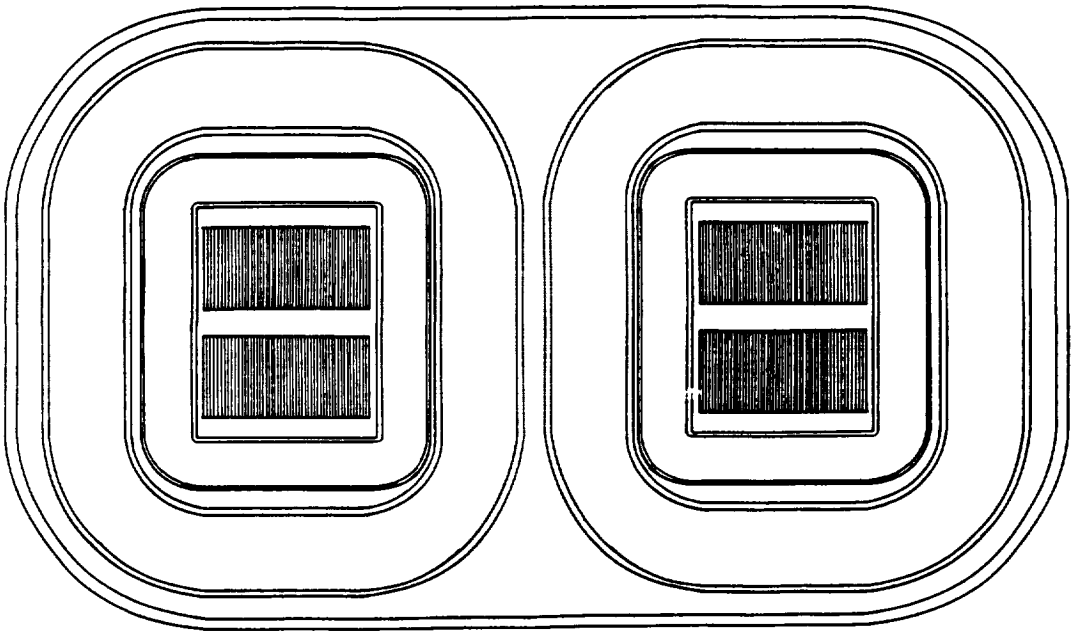

Figure 3.2.5-2. Section of transformer.

Basic Parameters

Design frequency	20,000 Hz
Coolant inlet temperature	300 K (27 °C)
Primary voltage (square wave)	5,000 V
Secondary voltage (square wave)	100,000 V
Primary current (sine wave)	126.5 A rms
Secondary current (sine wave)	23 A rms
Estimated per unit regulation	0.1
Primary coil voltage to ground	5,000 V
Secondary coil voltage, first layer to ground	10,000 V
Secondary coil voltage, last layer to ground	100,000 V
Design flux density (average over section)	0.8 T

Copper Conductors

Design current density	2400 A/in^2
Electrical resistivity	1.724E−6 ohm-cm at 20 °C
Temperature coefficient of resistance	0.00393
Specific gravity	8.96 g/cm^3
Thermal conductivity	394 W/m.K
Specific heat	0.091 cal/g.K (0.382 J/g.K)

Coil Insulation

All solid insulation (coil form, interlayer, intercoil, cover) is assumed to be fabricated of a material such as polypropylene, for which a design gradient of 800 kV/cm (2 kV/mil) is assumed.

Dielectric constant	2.3
Specific gravity	0.9 g/cm^3
Thermal conductivity	0.117 W/m.K
Specific heat	0.5 cal/g.K (2.093 J/g.K)
Design voltage gradient	2000 V/mil
Creepage field gradient (interlayer)	20 V/mil

Core Parameters

Core material	Metglas 2605S-3A
Specific gravity	7.29 g/cm^3
Thermal conductivity	9.0 W/m.K
Specific heat	0.13 cal/g.K (0.544 J/g.K)
Stacking factor	0.75
Flux density (in iron)	1.076 T
Flux density (average over section)	0.807 T
Core section width	D = 1 in × 2 = 2 in
Core section build	E = 2 in
Core window height	F = 4 in
Core window breadth	G = 6 in

Volts/layer	2500 V
Turns/layer	15
Number of layers	11
Layer winding height space factor	0.85
Height build of winding	0.89 in
Mean turn length	21.0 in
Total conductor length	3465 in
Dc winding resistance	0.305 Ω at 27 °C
R(ac)/R(dc) for coil winding resistance	1.367
Ac winding resistance	0.417 Ω at 27 °C
Conductor loss	221 W at 27 °C
Weight of conductor	4754 g
Layer insulation breadth	5.61 in
Layer insulation thickness	6 mil (3 wraps x 2 mil)
Inner coil insulation thickness	6 mil (3 wraps x 2 mil)
Outer coil insulation thickness	50 mil

Overall Parameters

Leakage inductance referred to primary	36 μH
Ac resistance referred to primary	9.211 m-Ω at 27 °C
Coil loss density	0.134 W/cm^3 at 27 °C
Average radial thermal conductivity of coils	0.158 W/m.°C
Heat transfer through cover insulation	92.3 W/m^2.K (0.0595 W/in^2.K)
Total coil loss	676 W at 27 °C
Total coil and core loss	4506 W at 27 °C
Total conductor volume	107.6 in^3
Total conductor weight	15800 g
Total conductor thermal capacitance	6030 J/K
Total insulation volume	31.4 in^3
Total insulation weight	464 g
Total insulation thermal capacitance	846 J/K
Total coil and core volume	244 in^3
Total coil and core weight	25684 g
Total coil and core thermal capacitance	12000 J/K

Package Parameters for Cooling Fluid in Tank

Overall dimensions of transformer tank	13.25 x 8.0 x 10.75 in
Total volume of transformer	1140 in^3
Volume of tank material (0.125 in thick)	81.5 in^3
Weight of tank (aluminum)	3609 g
Thermal capacitance of tank (Al)	3248 J/K
Volume of fluid in tank	814 in^3
Duct width	5.0 mm
Duct length	0.15 m
Total breadth of ducts	1.5 m
Hydraulic diameter	9.97 mm
Length-to-diameter ratio	15.0

Viscosity	8.96E−3 g/m.s
Prandtl number	0.706
Weight of hydrogen	4.36 g
Thermal capacitance of hydrogen	62 J/K
Total transformer weight	26748 g
Total transformer thermal capacitance	14035 J/K
Adiabatic temperature rise (average, 1000 s)	321 K
Velocity of flow	30 m/s
Reynolds number	10926.
Fanning factor, smooth duct	7.55E−03
Fanning friction factor	7.77E−03
Stanton number	3.05E−03
Heat transfer coefficient	429 $W/m^2.K$ (0.277 $W/in^2.K$)
Pressure drop	68.9 N/m^2 (10E−3 lb/in^2)
Volumetric flow	0.225 m^3/s (477 CFM)
Mass flow	73.7 g/s
Blower power	15.5 N.m/s = W
Fluid temperature rise	4.3 K
Inlet temperature	298 K
Outlet temperature	302 K
Average surface temperature rise	23.4 K
Core surface temperature rise	66 K
Core hot-spot temperature	391 K (118 °C)
Heat transfer through coil cover & surface	75.9 $W/m^2.K$ (0.0489 $W/in^2.K$)
Coil cover and surface temperature rise	28 K
Coil hot-spot temperature rise (from bulk gas)	114 K
Coil hot-spot temperature	414 K (141 °C)
Coil average temperature	385 K (112 °C)
Loss multiplier due to increase in resistance	1.34
Coil loss at average temperature	906 W
Total transformer loss at average temperature	4736 W

Summary

The temperature rise calculations are for continuous operation at full power. In view of the orbital duty cycle of 18.5%, the results are conservative. The temperature can be reduced by lowering the inlet temperature of the cooling fluid. In the case of oil cooling, this strategy is limited by a significant increase in its viscosity. Also, the heat transfer can be improved by increasing the fluid flow rate, if necessary.

The change from oil to hydrogen cooling increases the core hot-spot temperature from 62 to 118 °C, but the latter is still below the limit of 150 °C for Metglas 2605S-3A material. The increase in the coil hot-spot temperature from 135 to 141 °C is much less, because the poor thermal conductivity of the coil and high-voltage cover insulation is much more significant in determining the temperature rise.

In the case of oil cooling, if it is assumed that the weight of liquid surrounding the rectifier and filter capacitors (which are also oil cooled in this concept) and in the oil-to-hydrogen heat

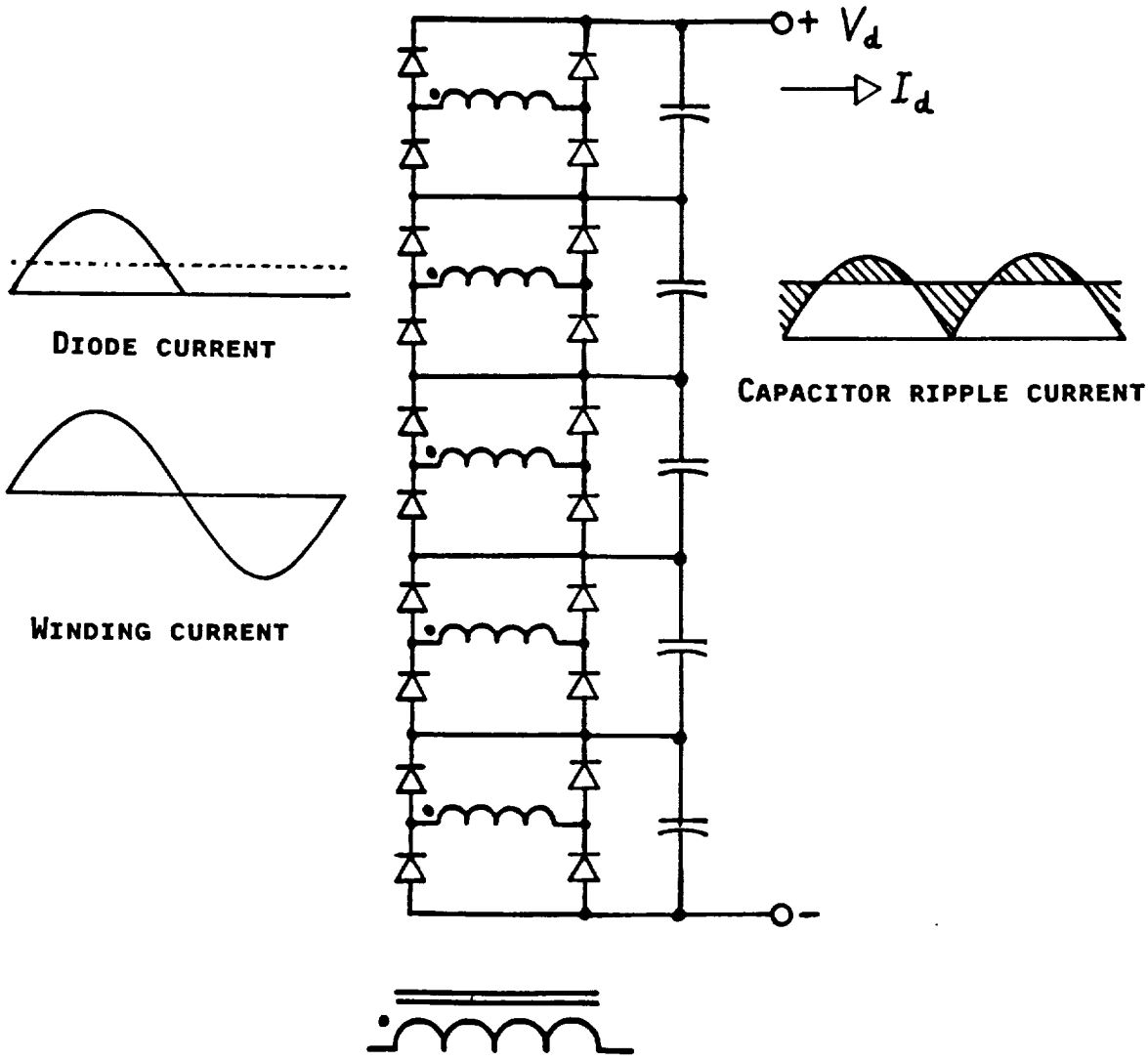

Figure 3.3.1-1. Full-wave bridge rectifier (drawn for N = 5 sections).

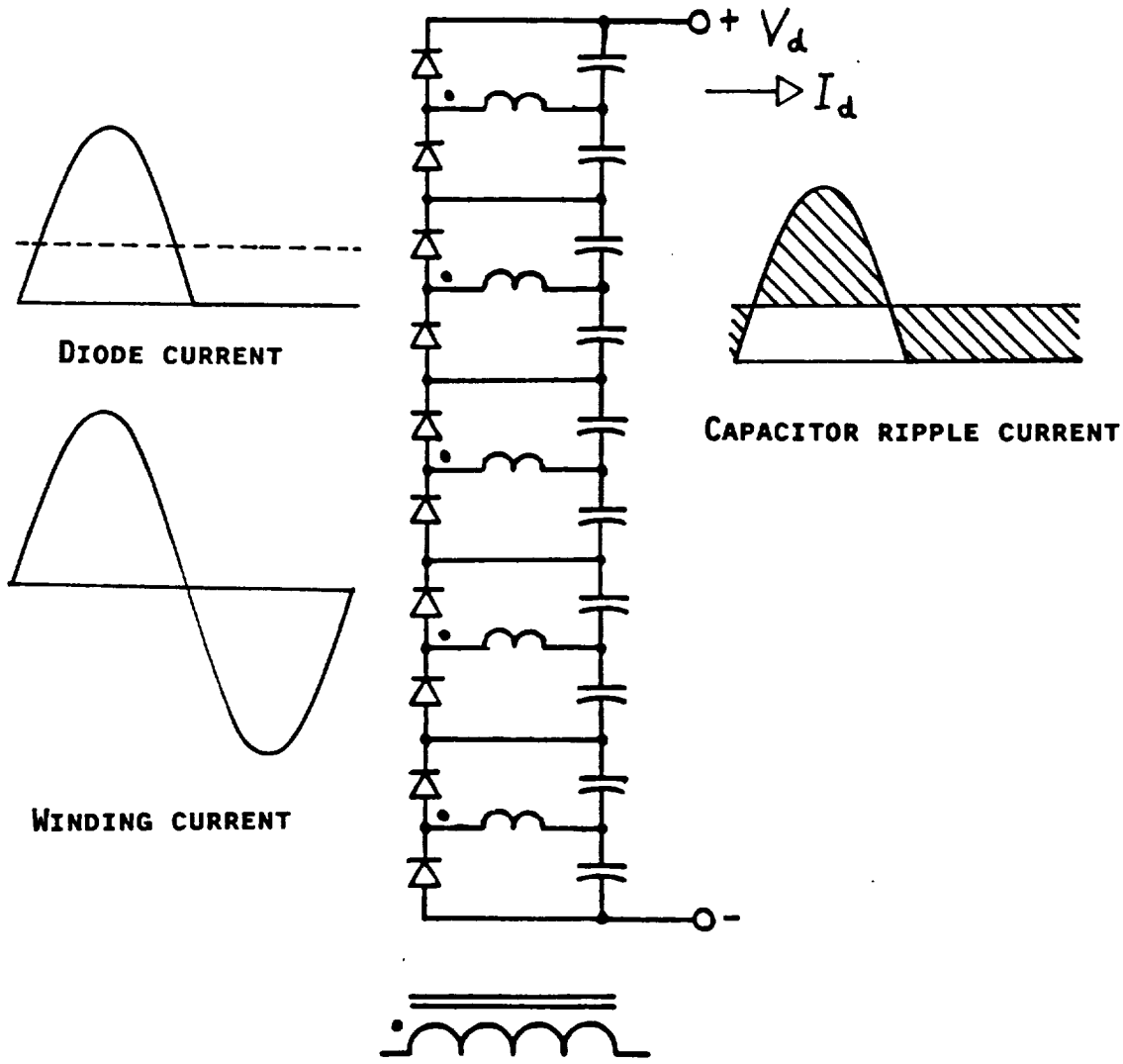

Figure 3.3.2-1. Half-wave bridge (voltage doubler) rectifier (drawn for N = 5 sections).

Capacitor Modules

The 80-nF, 100-kV dc filter capacitor will be divided into 22 series sections of 1.76 μF, 4.55 kV each. The total capacitor weight is estimated to be 14 kg, and the total loss 60 W. The capacitors will be manufactured by Maxwell Laboratories, and some details are given in Section 4.4.6.

3.4 Resonant Component Designs

3.4.1 Resonant Inductor Design

The series resonant inverter proposed for the 1-MW inverter requires that a resonating inductor be placed in series with the resonating capacitor and the transformer primary. The electrical parameters of this inductor are

Inductance	300 μH
Current (worst case)	235 A rms (at 22 kHz)
Peak voltage	18800 V (at 1 MW load)
Q	> 500

The present design of the inductor uses a two-C-core configuration. The copper wire is wound over the gaps of the core. Figure 3.4.1-1 shows the configuration and size of the inductor design. The copper conductors are electrically isolated from the core material by two polypropylene bobbins, one over each gap.

The inductor core consists of a cut, tape wound core material. There are two possible materials for the core: Allied amorphous 2605-S3A, and Hitachi Finemet.

Figure 3.4.1-2 shows the design parameters for the resonant inductor. The parameters listed are for Allied 2605-S3A core material. The values in parentheses are for Hitachi Finemet core material. The inductor loss, at 1-MW load, is 2700 W using the amorphous core material (2605-S3A) and 1800 W using the new Finemet material. The mass of the inductor using 2605-S3A is 10.1 kg; using Finemet it is 10.2 kg.

Figure 3.4.1-3 shows the magnetic flux pattern of the inductor. The finite element software package used to generate this pattern was GE2D. The figure shows that the flux is well contained within the core material. There is very little fringing flux for this design, resulting in low proximity loss and mimimal magnetic coupling to the local environment. Also, the Q of this inductor design is high. An option for Phase 2 of the program is to design the resonant inductor using a low-permeability (e.g., 10) core material with no gap. Such a design will adequately keep the flux within the core to minimize flux fringing loss. Conversations between GE and magnetic vendors will be pursued for this option using alternative magnetic materials including flake materials.

3.4.2 Resonant Capacitor Design

The values for the resonant components were chosen to obtain a high degree of control of the output voltage, while not placing an excessive voltage and current burden on these components.

The resonant capacitor is 200 nF, and handles a maximum steady-state current of 235 A (rms) at 22 kHz while experiencing a maximum steady-state voltage of 12,000 V (peak). During a fault condition, a maximum of 25000 V peak can occur, but the fault will disable the inverter within 1 ms. The rms current rating of the capacitor is not significantly affected by the short duration of increased current. The control circuit provides an inherent peak voltage lim-

Core Material – Allied (Hitachi)	2605S–3A (FINEMET)
Core size	16.5x16.5x5.25 cm 6.5x6.5x2.1 in
Core loss (at 1 MW, 20 KHz, steady state)	1900 W (1000 W)
Copper wire I ^ 2*R loss (steady state, 233 Amps rms)	300 W
Copper wire proximity loss (steady state, 233 Amps rms)	500 W (est)
Core mass	8.9 kg (9.0 kg)
Copper wire mass	1.2 kg
Copper wire area (per single conductor)	.13 cm ^ 2 .02 in ^ 2
Copper wire Rac/Rdc (at 20 KHz)	1.35
Copper wire current density (at 20 KHz, 233 Arms)	2440 A/cm ^ 2
Core material peak induction (20 Khz, 233 Arms)	1.2 Tesla
Core material saturation induction	1.41 Tesla (>1.35 Tesla)
Core material electrical conductivity	7.25*10 ^ 5 S/m (9.1*10 ^ 5 S/m)
Core material skin depth (at 20 KHz)	.0183 mm, .72 mil (.025 mm , .99 mil)
Curie temperature	358 'C (570 'C)
Total Core Loss	**2700 Watts** **(1800 Watts)**

Figure 3.4.1-2. Resonant inductor design parameters.

itation on the resonant capacitor. The maximum capacitor fault voltage can be reduced below the 25 kV (peak) through the design of the control section.

3.4 Control System Design and Simulation

The anticipated applications of these high-power converters involve two major modes of control:

1. Dc voltage regulation with current limit, for ordinary power supplies to feed variable-current loads.
2. Dc current regulation with voltage limit, for charging energy-storage capacitors used in pulse-forming networks (PFNs).

To obtain either mode of control, we expect to use both frequency modulation and phase control (pulse-width modulation) for the resonant inverter.

One of the main issues with this converter is the very high voltage (100 kV) at the output. Sensing this value can be accomplished by a frequency-compensated voltage divider. This lower level signal will require isolation before it can be connected to the integrated control circuit. With a system power rating of up to a megawatt, current limit is necessary to prevent damage caused by high-voltage arcs and fault currents.

3.4.1 Series-Resonant Circuit Characteristics

The circuit topology for this report is a series super-resonant inverter, so named because the frequency of operation is always greater than the resonant frequency. Series super-resonant circuit operation has the advantages that no power switch turn-on loss occurs, loss-less capacitive snubbing can be used, and overall circuit efficiency is high. Reduced electrical stress on the semiconductor devices and reduced EMI occur because of the near-sinusoidal current waveform. Figure 3.5.1-1 shows the circuit schematic and the component values. The circuit switches at high frequency in order to reduce the size and weight of the principal components.

The circuit is termed series resonant because the resonant inductor (L_{res}), and resonant capacitor (C_{res}) are in series with the primary of the high-voltage transformer. The resonant frequency for the circuit of Figure 3.5.1-1 is 20.5 kHz ($1/[L_{res}*C_{res}]^{1/2}$) and is an important circuit characteristic.

The computer analysis in this section assumes ideal switches. The actual semiconductor switching device used will be the MCT (shown for simplicity as a bipolar transistor). Each of the transistors of Figure 3.5.1-1 turns on switches independently. The only constraint on the circuit is that devices Q1 and Q2 (or Q3 and Q4) cannot be turned on simultaneously to prevent shoot-through, a direct conduction path from the dc supply bus to common. The voltage across nodes A and B of Figure 3.5.1-1 can be either $+V_{rail}$, $-V_{rail}$, or 0 V, depending on which combination of transistors or diodes is conducting.

This circuit has three energy storage components: L_{res}, C_{res}, and C_{out}. The interaction of these energy storage components is critical to the operation and understanding of the circuit.

Frequency Modulation

The output voltage of the 100-kV filter capacitor is assumed to remain constant during a single steady-state switching event. This is a valid assumption, as shown by the maximum capacitor ripple of 0.25% (peak) from the simulation results. The filter capacitor output voltage

reflects back to the primary of the transformer as $+Vc_{out}/N$ when IL_r is positive, and $-Vc_{out}/N$ when IL_r is negative.

Using frequency modulation, the switch pair Q1 and Q4 (or Q2, Q3) are gated on and off simultaneously. The pair Q1:Q4 remains on for 50% of the time, and Q2:Q3 on for the other 50%. The duty ratio always stays at 50%. The frequency of the gating signals changes to regulate the output voltage under different load conditions.

For inverter operation above resonance, an anti-parallel diode (coasting diode) turns on before its corresponding transistor turns on. This action discharges the snubber capacitor (not shown in Figure 3.5.1-1) and recovers the capacitor energy. The diode does not need to be a fast recovery type, and the system exhibits lossless snubbing.

The steady-state operating condition of the series super-resonant inverter sequences through a four-mode cycle. Figure 3.5.1-2 displays these modes. The inverter cycles through mode 1, mode 2, mode 3, mode 4, mode 1.... The dark lines show the current path for that mode. Figure 3.5.1-2 displays the conducting semiconductor devices, the voltage applied across the resonant network, and the direction of current.

Figure 3.5.1-3 displays the resonant inductor current and resonant capacitor voltage waveforms during a 1-MW, steady-state operating condition. The figure displays the conduction region of each of the semiconductor devices. The output voltage reflects back to the primary of the transformer as a dc voltage of value $+Vc_{out}/N$ or $-Vc_{out}/N$. Using this, and the polarity of the applied rail voltage (depending upon which semiconductor devices are conducting), the four conduction modes comprise the resonant capacitor and inductor in series with four discrete voltage source values. The resulting resonant inductor current and resonant capacitor voltage consist of sections of sinewaves for each of the four modes. Only the applied forcing function is changing in a stepwise fashion.

It is important to note that this analysis transforms the initial nonlinear system into a linear equivalent model. The control method described later uses this linearization property.

Figure 3.5.1-4 displays the equivalent resonant-network circuit. The applied voltage (V_{ab}) is a variable frequency square wave. The figure shows a loss component resistor including copper losses, I^2R losses, etc. The series resonant network has an output voltage transfer function shown in Figure 3.5.1-5. The x-axis is the frequency of the applied square wave, and the y-axis is the output voltage. The regulated output voltage is 100 kV for the NASA inverter. The figure has a horizontal line drawn at 100 kV, with a vertical line at the 20.5-kHz resonant frequency of the network. Since the network is super-resonant, it always operates to the right of this vertical line. The applied voltage V_{ab} is always at a frequency greater than 20.5 kHz. A locus of four output currents (0.5, 2.5, 5, and 10 A) displays the transfer function of the inverter for each current.

At high output currents, the slope of the transfer function ($\Delta Vc_{out}/\Delta freq$) is large. The 100-kV output voltage operating point is at the intersection of the current locus line and the 100-kV line. For super-resonant operation, to keep the output voltage constant, the operating frequency increases as the load current decreases. For very low current conditions, the switching frequency is too high for the semiconductor switches. For the 0.5 A load current condition of Figure 3.5.1-5, the operating frequency of the semiconductor switches would need to be much greater than 50 kHz. The control system must use another method to regulate the output voltage under low-load current conditions.

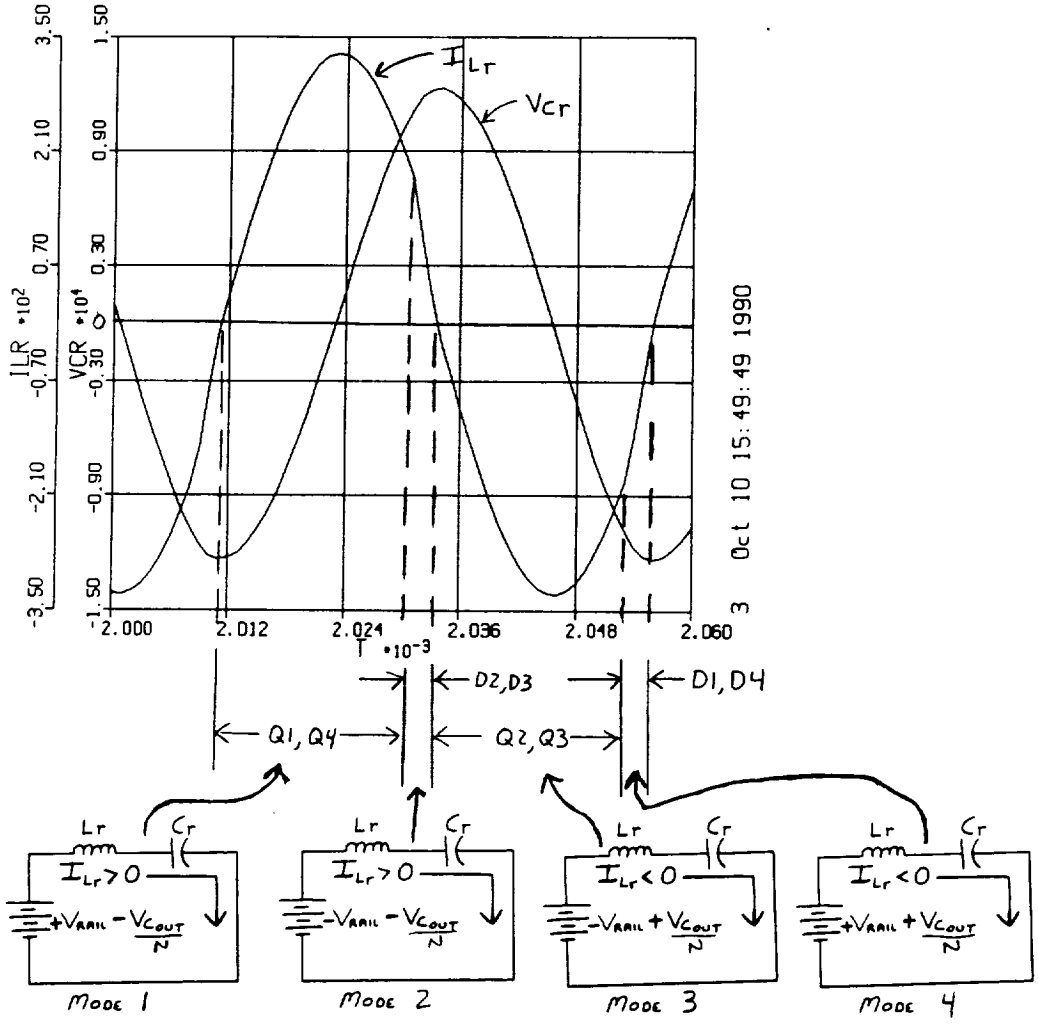

Figure 3.5.1-3. Conduction intervals, and equivalent circuit.

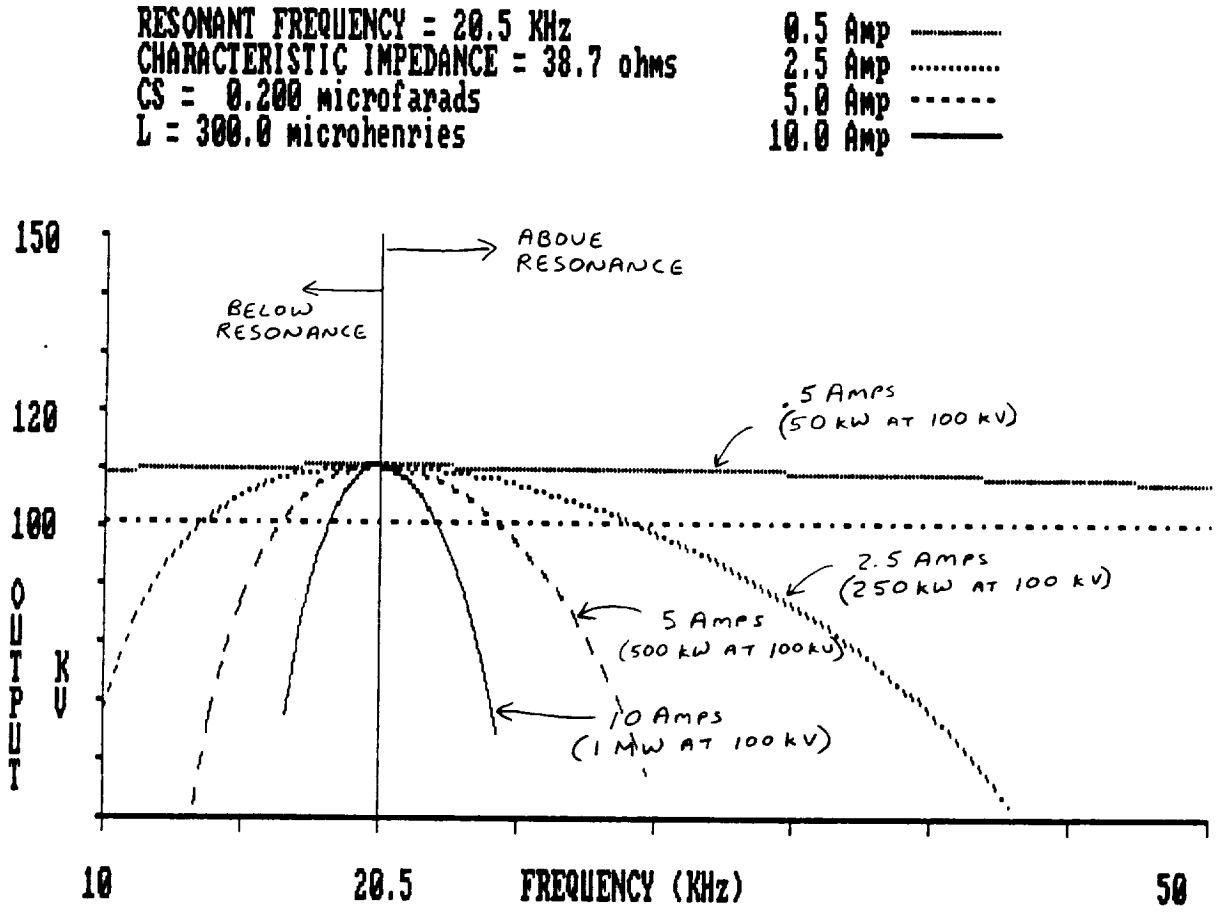

Figure 3.5.1-5. Transfer function using frequency modulation.

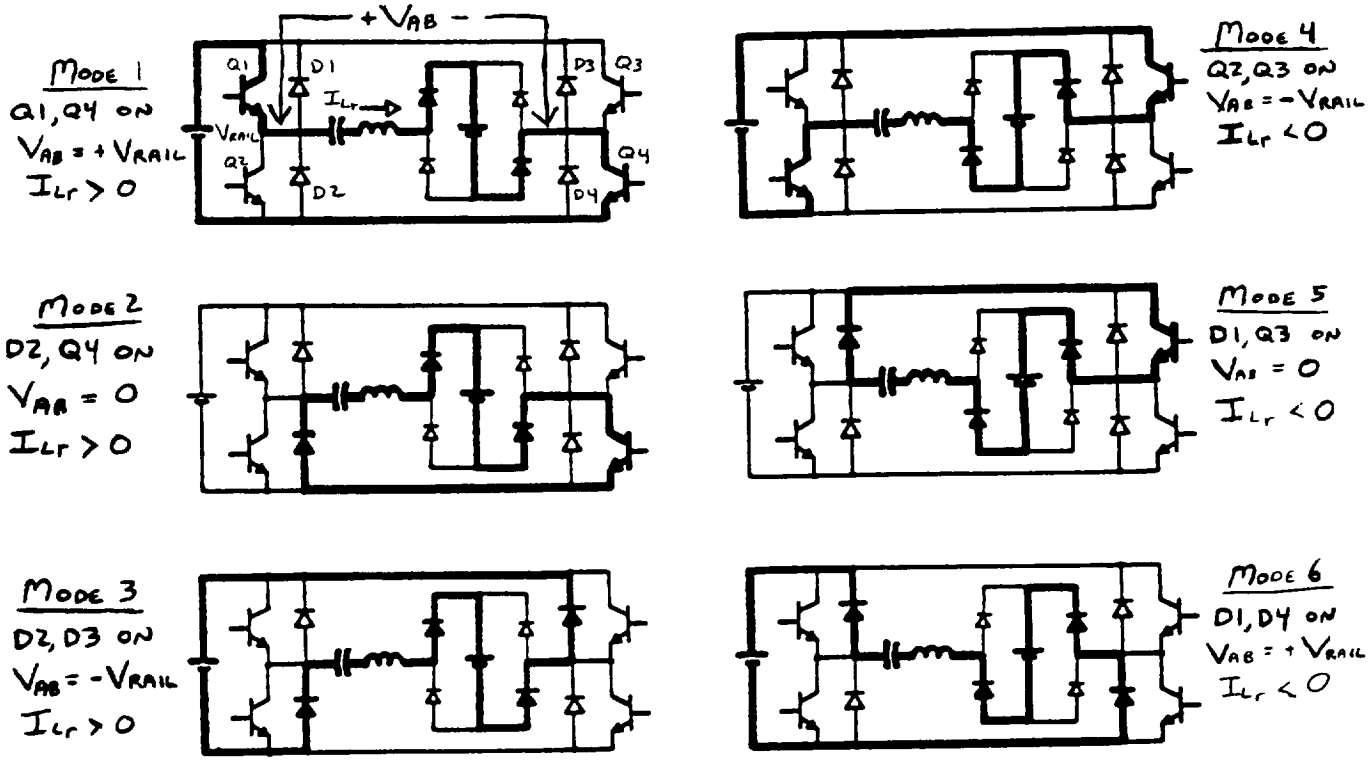

Figure 3.5.1-6. Sequence for phase modulation.

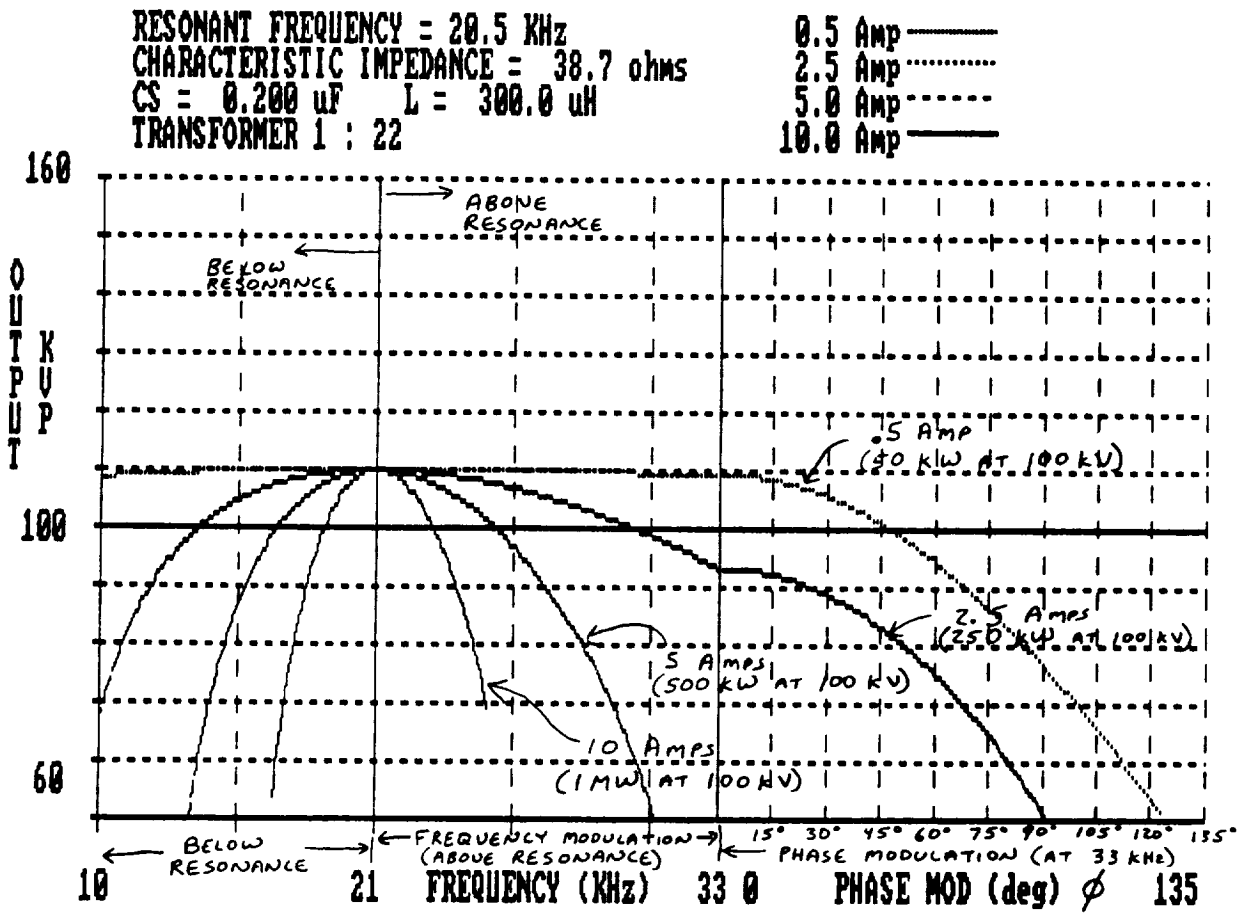

Figure 3.5.1-8. Transfer function using frequency/phase modulation.

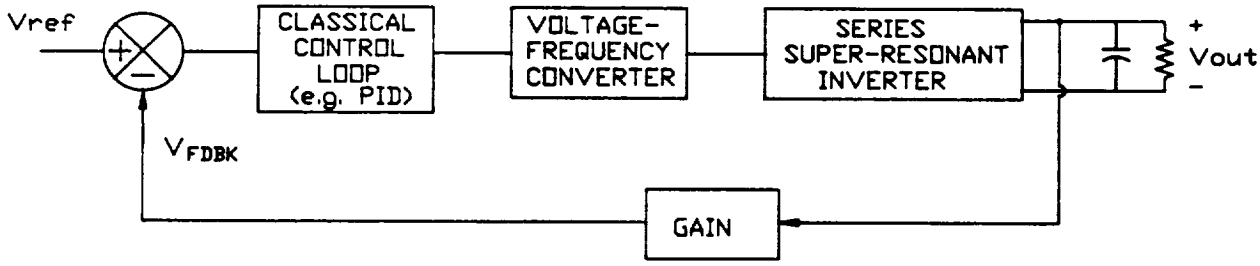

Figure 3.5.2-1. Common control method used for resonant inverters.

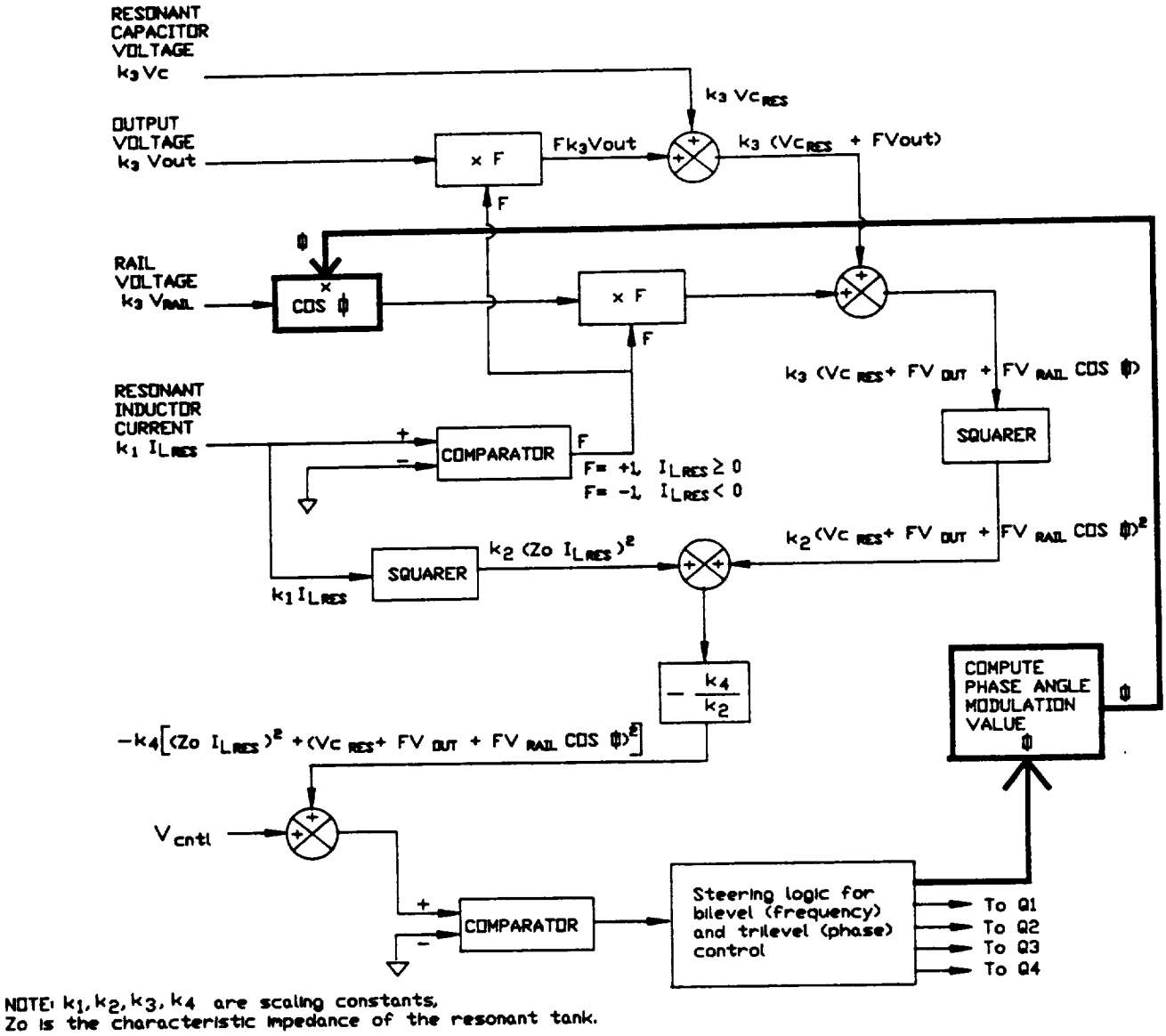

NOTE: k_1, k_2, k_3, k_4 are scaling constants,
Zo is the characteristic impedance of the resonant tank.

Figure 3.5.2-2. Modified optimal control block diagram.

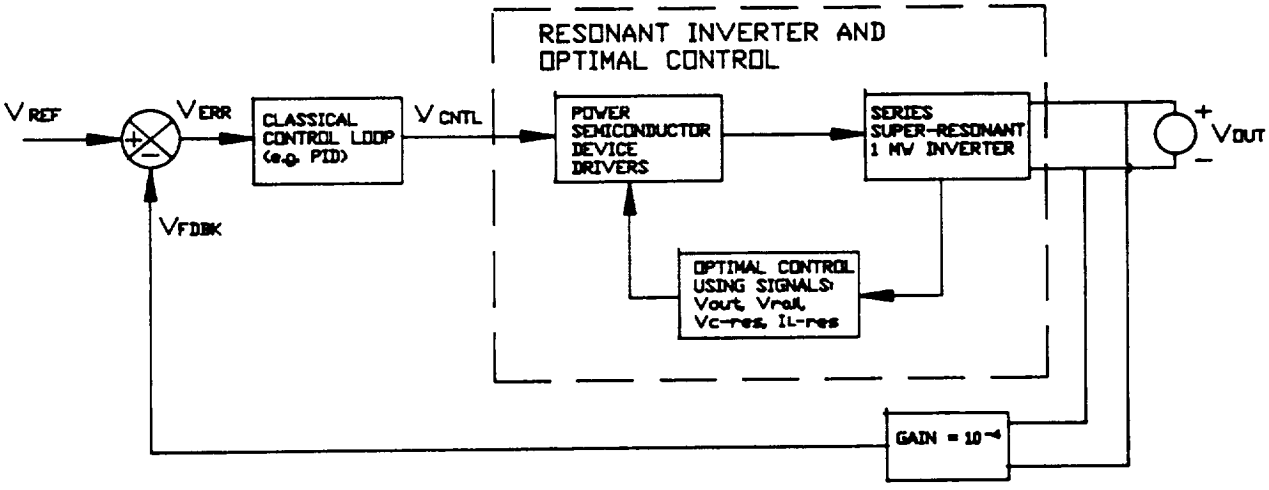

Figure 3.5.2-3. Closed loop control for series super-resonant inverter.

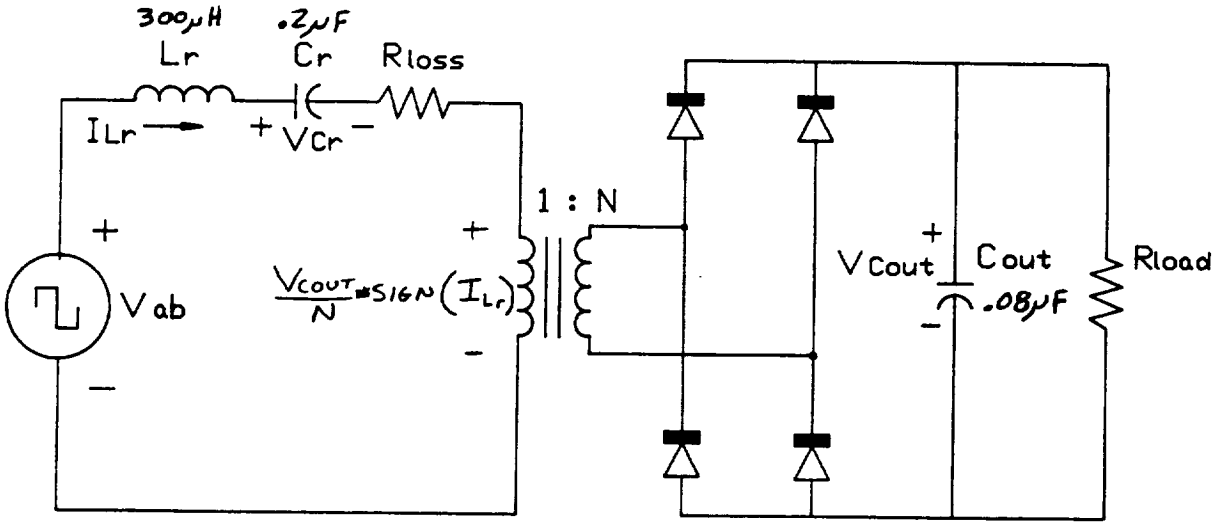

STATE EQUATIONS

$$\dot{I}_{Lr} = [1/Lr]\,[V_{appl} - V_{Cr} - I_{Lr} * R_{loss} - sign(I_{Lr}) * V_{Cout}/N]$$

$$\dot{V}_{Cr} = [1/Cr]\,[I_{Lr}]$$

$$\dot{V}_{Cout} = [1/C_{out}]\,[ABS(I_{Lr})/N - V_{Cout}/R_{load}]$$

NOTE: This system is nonlinear due to the ABS and Sign functions.

Figure 3.5.3-1. Inverter and state equations.

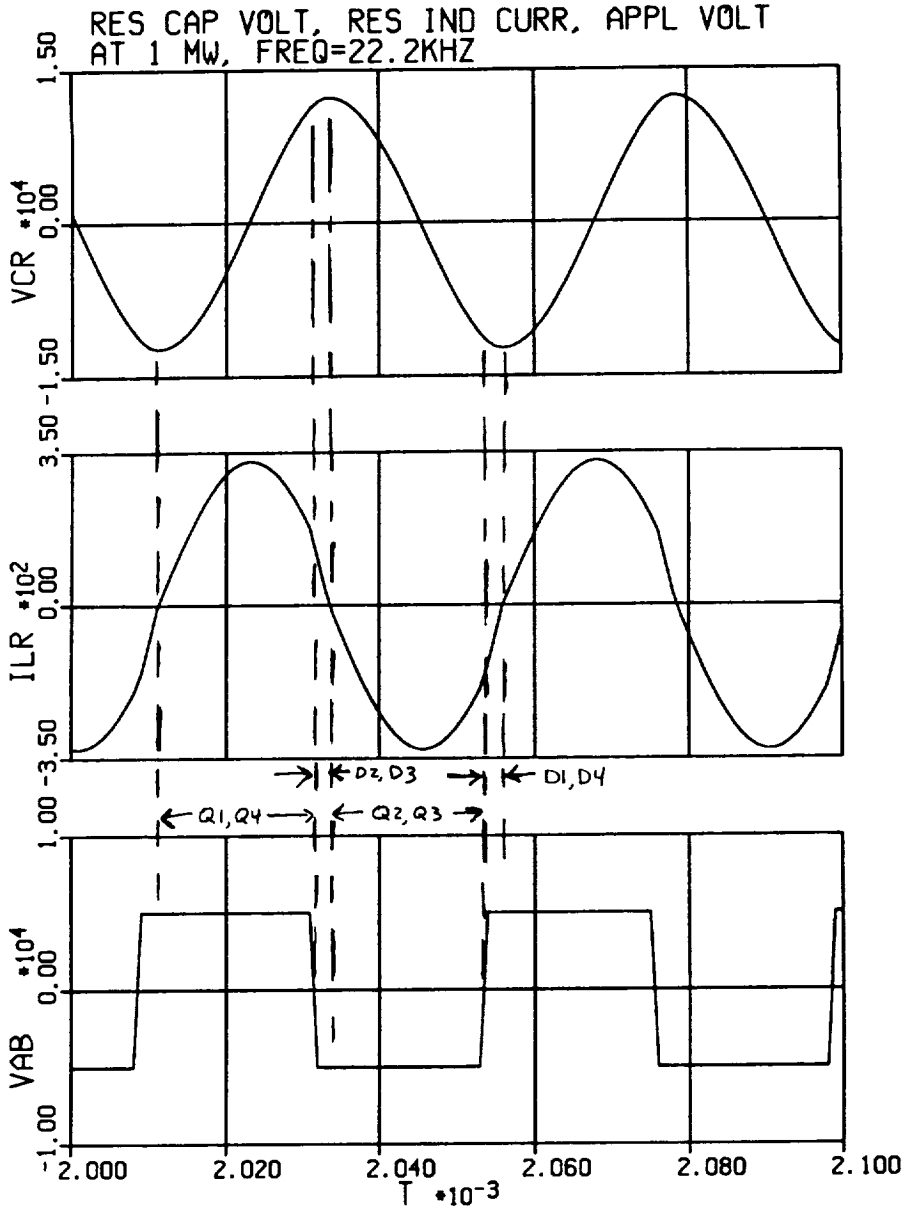

Figure 3.5.3-4. Inverter waveforms – 1-MW load.

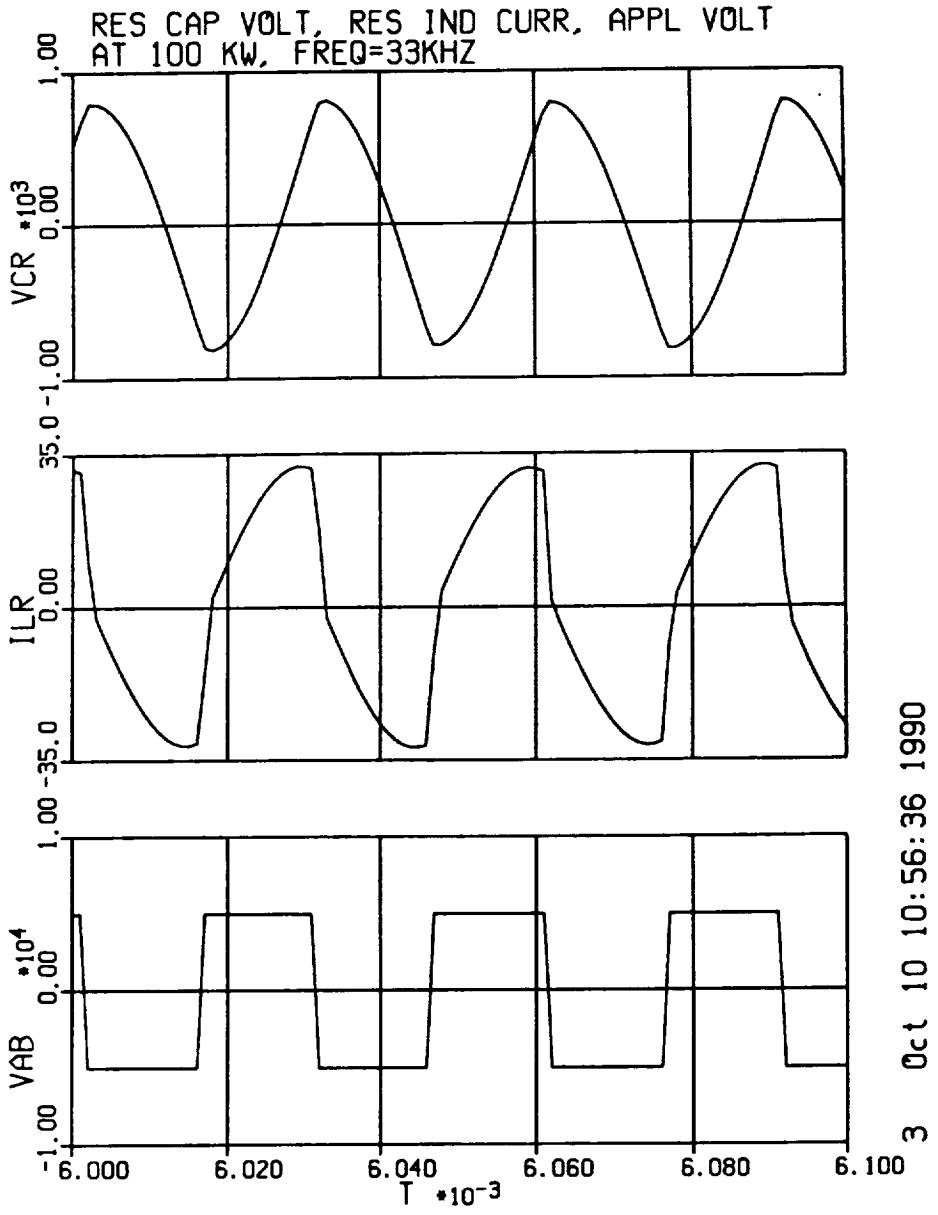

Figure 3.5.3-7. Inverter waveforms – 100-kW load.

ure 3.5.3-9. The implementation of the short-circuit protection is to place a limit (i.e., a clamp) on the control signal of the modified optimal control (Figure 3.5.2-2). The magnitude of the short-circuit current depends upon the clamp value. This limit controls the maximum output current delivered under a fault condition and the stress placed on the inverter electronics.

Figure 3.5.3-9 shows the system response when powered to a 1-MW steady-state condition (R_{load} = 10K). A "short-circuit" load condition, simulated by a 100-Ω load resistance, is applied at 3.5 ms. The 100-Ω short-circuit value was chosen to be 1% of the smallest operating load (1 MW corresponds to 10000 Ω). Choosing a resistance value less than this does not alter the output current or electrical stress to a significant extent. The commanded voltage reference remains at 100 kV; however, the inverter control limits the output current to approximately 20 A at a reduced output voltage of 2 kV. The inverter can continue to operate at this output short-circuit condition for several milliseconds without damage to any components. The control limits the peak capacitor voltage and inductor current. However, the circuit must be disabled before the components heat up beyond their rated specifications.

Figure 3.5.3-10 displays the resonant capacitor voltage and resonant inductor current for the short-circuit condition of Figure 3.5.3-9. The initial transient (0 to 0.6 ms) occurs during the interval when the control is bringing the output voltage up to 100 kV. At 3.5 ms the short-circuit fault occurs. The current and voltage is bounded to a larger value. The magnitude of the voltage and current during the short circuit is controlled by the clamp value placed in the control circuitry. The inverter control circuit (i.e., low voltage, low power electronics) provides this short-circuit protection; no high-power protection circuit is needed to protect the inverter and its components during this fault. The fault eventually must be removed, or the inverter must be disabled before the inverter components overheat, but the circuit has a relatively long time interval (i.e., several milliseconds) before this would occur.

3.6 System Protection

The converter system must be protected against load faults, source faults, and internal converter faults. The most critical component of the converter to be protected is the semiconductor switch module, which is also the component most capable of rapid response to fault conditions. The control circuit of the inverter switches will incorporate as many features as possible, such as current limiting, automatic shutdown, and careful restarting, to protect the load and source as well as self-protection of the switches. This will be the first line of protection, and should be sufficient for the load, assuming it is not regenerative.

The second line of protection will be the dc input circuit fuse. For a 1-MW converter module, the fuse must be rated for 5 kV, 200 A, and must operate as fast as possible. The dc input filter inductance will limit the rate of rise of fault current, but the steady fault current will be determined by the characteristics of the dc source. The minimum function of the fuse will be to isolate a failed converter module. The desired function will be to protect the MCT switches in case of misfire or accidental conduction of a pair of switches in the same phase leg (shoot-through).

Typical high-voltage loads are subject to short-circuit faults, and might be damaged by discharge of the output filter capacitors, which store 400 J in our present design. For protection, a crowbar consisting of a triggered spark gap is proposed. This equipment will be supplied by Maxwell Laboratories, and the arrangement is described in detail in Section 4.4.7. The weight is estimated to be 1.84 kg.

3.7 Cooling System

A scheme for direct hydrogen cooling of the entire converter system is outlined in Figure 3.7-1. The components are mounted within a common, thin-walled enclosure containing hydrogen under a static pressure of about 4 atm, which need not be maintained when the converter is not operating. However, it is assumed that the temperature is maintained within a range between about 270 and 310 K (−3 °C to 37 °C), compatible with the optimum storage temperature of all components, under standby conditions.

In operation, hydrogen is blown through the enclosure to cool the components, maintaining a continuous circulating loop (Figure 3.7-1). As the gas becomes heated above a certain temperature limit (310 K, for example), some of it is exhausted from the outlet end of the system and replaced by injecting fresh liquid hydrogen at 20 K into the cooling loop. The fresh hydrogen is evaporated and mixed with the circulating flow to reduce the inlet temperature to a certain lower limit (270 K, for example). The blower may be located at either the inlet end, as shown in the figure, or at the outlet end. Appropriate temperature and pressure controls are provided for the blower and the inlet and outlet valves.

In steady-state operation, the amount of hydrogen injected as a liquid at 20 K is equal to the amount exhausted as a gas at 310 K. This allows all the enthalpy of hydrogen over this temperature range to be utilized for cooling the converter, minimizing the quantity required. The average specific heat of gaseous hydrogen over this temperature range is about 12.75 J/g.K, so the heat absorption capacity is

$$Q_{gas} = (310 - 20) \times 12.75 = 3697 \text{ J/g}$$

To this, the latent heat of vaporization (1831 J/g) can be added:

$$Q_{total} = 3697 + 1831 = 5528 \text{ J/g}$$

The hydrogen mass flow required for continuous operation is then

$$H_2 \text{ flow} = \frac{3600}{5528} = 0.65 \text{ kg/kWh}_{loss}$$

$$= 36 \text{ kg/h} \quad \text{for 56 kW loss}$$

In the gas circulating loop, the specific heat of hydrogen at the average temperature of 290 K (17 °C) is 14.3 J/g.K, so the heat absorption capacity from 270 K to 310 K is

$$Q_{loop} = (310 - 270) \times 14.3 = 572 \text{ J/g}$$

The hydrogen mass circulating flow required is then

$$H_2 \text{ circulating} = \frac{1}{572} \text{ g/J}_{loss}$$

$$= 98 \text{ g/s} \quad \text{for 56 kW loss}$$

The blower power required to maintain this flow is estimated to be about 1 kW. The particular temperatures assumed in these calculations may be modified to optimize the operating temperatures of the components.

3.8 Summary

The design of the high-voltage transformer-rectifier has been established. A core-type structure employing two coils, one on each leg of a C-core, has lower weight than the alterna-

tive shell-type structure, with a single coil on one leg of the core, or on the center leg of an E-core. The primary windings are connected in parallel, which balances the flux in each leg. A special interconnection between the secondary windings and the rectifier and filter is needed to minimize reflected capacitance at the primary side. The secondary windings are divided into sections, each consisting of a single layer from each coil connected in series, and each feeding a section of the rectifier. By making series connections of these sections on the dc side, the interlayer voltage is purely dc (equal to the output voltage divided by the number of sections). Thus, the charge on the interlayer capacitance does not have to be cyclically reversed, thereby reducing the effective ac capacitance to a very low value. This is required for proper operation of the series inverter. A half-wave bridge (voltage doubler) rectifier connection has been selected because it can be built with fewer sections or layers (11 in the proposed design) than a full-wave bridge. This reduces the amount of layer insulation and the number of leads required, as well as the number of diode modules.

Some type of amorphous metal (Metglas or Finemet) will be used for the core. While our present design uses Metglas 2605S-3A operating at about 1 T, this is subject to more detailed evaluation of materials and the variation of core loss with flux density. A critical factor in minimizing transformer weight is achieving a high conductor-to-insulation space ratio, especially in passing through the core window. Both primary and secondary windings will employ copper conductors of rectangular compacted litz wire, needed at 20 kHz. The high-voltage secondary windings will be completely enclosed within solid insulation forms of a material such as polypropylene, across which a very high voltage gradient can be allowed. Sections of the coil forms must fit together very tightly so that the high-gradient electric field is contained within the assembly, allowing close spacing to the core and nearby grounded structures. To remove the heat generated by losses when operating at high core flux density and high coil current density, cooling ducts will be provided in the structure, except in the core window.

In our original concept, the rectifier diodes and dc filter capacitors were to be enclosed with the secondary windings in extended forms of polypropylene insulation, and the assembly mounted together with the resonant inductor in an aluminum tank filled with oil for insulation and cooling. However, this plan was modified because of the disparity in the heat generation and temperature limits of these components, and it is now proposed to group the diodes and capacitors at one end of the transformer. In this arrangement, forced oil cooling will be effective but the weight of the oil and tank, as well as the weight of an oil to liquid hydrogen heat exchanger, imposes a severe penalty.

The use of direct gaseous hydrogen cooling is now proposed, eliminating the oil and allowing the tank to be replaced by a lightweight enclosure that includes the inverter and all other components. Estimates of the heat transfer obtainable with this system show that it is feasible and should save much weight, but the effect on the dielectric insulation system requires further study. At 4 atm, the breakdown voltage of hydrogen is about 50 kV/cm. Since the dielectric constant of hydrogen (1.0) is less than that of the oil (2.55) or the solid insulation (2.3), it will experience a higher electric field gradient. Reducing the electric field gradient requires a somewhat larger core and coil but the overall weight should be less than for an oil-cooled system.

The estimated weight and losses of the converter system components are listed in Table 3.8-1. The overall converter system efficiency is estimated to be 94.4%. To remove the 5.6% losses, hydrogen flow at 36 kg/h is required when operating at full power.

The resonant inductor design operates at a peak flux density of 1.2 T for the 1-MW load condition. The design of this core uses a C-C core configuration, which reduces stray flux and

3.9 References

[1] R. Oruganti and F.C. Lee, "Resonant Power Processors," *IEEE Trans. Ind. Appl. Vol. IA-21,* No. 6, 1985, "Part I - State Plane Analysis," pp. 1453-1460, "Part II - Methods of Control," pp. 1461-1471.

[2] R.J. King and T.A. Stuart, "Modelling the Full-Bridge Series Resonant Power Converter," *IEEE Trans. Aerosp., Vol. AES-18,* No. 4, 1982, pp. 449-459.

[3] W. McMurray, "The Thyristor Electronic Transformer - A Power Converter using a High Frequency Link," *IEEE Trans. Ind. Appl., Vol. IGA-7,* No. 4, July/August 1971, pp. 451-457.

[4] F.G. Turnbull and R.E. Tompkins, "Design of a Pulsewidth Modulated Resonant Converter for a High Output Voltage Power Supply," *IEEE Trans. Ind. Appl., Vol. IA-23,* No. 6, 1987, pp. 1016-1021.

[5] R.L. Steigerwald, "A Comparison of Half-Bridge Resonant Converter Topologies," *IEEE Trans. Power Electronics, Vol. PE-3,* No. 2, 1988, pp. 174-182.

[6] R. Oruganti, J.J. Yang, and F.C. Lee, "Implementation of Optimal Trajectory Control of Series Resonant Converter," *Conf. Rec. IEEE-PESC,* 1987, pp. 451-459.

[7] R.J. King and T.A. Stuart, "Inherent Overload Protection for the Series Resonant Converter," *IEEE Trans. Aerosp., Vol. AES-19,* No. 6, 1983, pp. 820-830.

[8] P.L. Dowell, "Effects of Eddy Currents in Transformer Windings," *Proc. IEE, Vol. 113,* No. 8, August 1966, pp. 1387-1394.

[9] E.C. Snelling, *Soft Ferrites - Properties and Applications,* Second Edition, London, England: Butterworth & Co., 1988.

[10] "High-Frequency Ferrite Power Transformer and Choke Design Series," *Philips Technical Publications 205-208: Part 3. Transformer winding design (207).*

[11] M.M. El-Missiry, "Current Distribution and Leakage Impedance of Various Types of Foil-Wound Transformers," *Proc. IEE, Vol. 125,* No. 10, October 1978, pp. 987-992.

[12] P.D. Evans and K.H. Al-Shara, "Losses in Foil-Wound Secondaries in High-Frequency Transformers," *IEEE Trans. Magnetics, Vol. 25,* No. 4, July 1989, pp. 3125-3132.

[13] "Hitachi New Soft Magnetic Materials 'FINEMET'," Hitachi Metals, Ltd., YA-880901.

[14] H. Fukunaga, T. Eguchi, K. Koga, Y. Ohta, and H. Kakehashi, "High Performance Cut Cores Prepared from Crystallized Fe-Based Amorphous Ribbon," *IEEE Trans. Magnetics, Vol. 26,* No. 5, September 1990, pp. 2008-2010.

[15] M. Jakob, "Influence of Nonuniform Development of Heat Upon the Temperature Distribution in Electrical Coils and Similar Heat Sources of Simple Form," *Trans. ASME, Vol. 65,* 1943, pp. 595-605.

[16] T.J. Higgins, "Formulas for Calculating the Temperature Distribution in Electrical Coils of General Rectangular Cross Section," *Trans. ASME,* Vol. 66, 1944, pp. 665-670.

[17] A. Rele and S. Palmer, "Cooling of Large Transformer Cores," *Trans. IEEE, Vol. PAS-91,* No. 4, July 1972, pp. 1527-1535.

Section 4

RESONANCE TRANSFORMER-BASED SYSTEM
(Maxwell Laboratories, Inc.)

4.1 Introduction

The high-power, high-voltage dc-dc converter program is intended to provide a power system for a variety of future high-power, space-based applications. The specifications describe a system that is well beyond the established state of the art for power converters. The fact that this system will operate in a space environment also has a strong influence on these specifications. System weight, cooling, and reliability are examples of parameters whose importance is magnified in a space-based power system of this power level. As a result, the system proposed to meet these requirements is different in many respects from conventional power converters.

Among the salient features of the resonance transformer-based system are

- The inverter uses MCTs as the switching element, which lowers the device count and the losses compared with other devices at the operating frequency of 50 kHz.
- The voltage step-up is accomplished by a resonance transformer, a Maxwell-patented resonant circuit. This circuit requires no magnetic materials, allowing for operation at higher inverter frequencies and for a simpler cooling scheme than conventional systems.
- The Maxwell capacitors used in the system have power densities well beyond that commercially available today.
- A regulator circuit developed at Maxwell provides output voltage regulation of ±0.25% or better with a bandwidth of greater than 1 MHz, and weighs less than 3 kg.

These features allow the resonance transformer-based system to meet or exceed the specifications desired for this program. This approach will also be shown to scale up to higher power densities as the output power level increases.

4.2 System Specifications

The requirements for the system are

Input voltage	5 kV dc
Output voltage	100 kV dc ±0.25%
System mass	< 100 kg
Duty	> 1000 s continuous operation
Fault energy to load	"a few tens of joules"

4.3 Critical System Issues

4.3.1 System Weight

The weight of the system is the most critical parameter of those listed above because it is the most difficult to meet. The power density of 0.1 kg/kW is well beyond the state of the art for current systems at this power level. The techniques used to meet this requirement include the use of cryogenic cooling of components, a new generation of high power density capacitors, a resonant voltage step-up circuit, a proprietary regulator design, and components espe-

that fault current. Fusing was chosen because fuses can be made much lighter than dc interrupters at this power level. While interrupters can operate repeatedly without replacement, it is questionable whether or not this is an advantage for this system. In a high-power system such as this one, the problem that originally caused the fault will most likely still be present in the system after the fuse or interrupter clears the fault, which means that repairs must be performed before the system is operational again. The fuse can be replaced when the rest of the system is repaired. For almost all forseeable fault scenarios, a fused disconnect has all the features of a dc interrupter, with the advantages of faster, more reliable operation and lighter weight.

A terrestrial 5-kV, 200-A fuse would be approximately $12 \times 12 \times 6$ in and would weigh more than 20 kg. This is unacceptably large and heavy for this system. Fortunately, the size and weight of the fuse can be reduced by cooling the conducting element. Liquid nitrogen cooling of wires has been investigated by Gilmour et al. [1] for fusing and current-limiting applications. The cryogenic liquid is boiled off the conductor by the heat generated in the conductor, forming a gas jacket around the wire and maintaining a constant temperature on the outside of the wire. At a certain critical temperature, the boil-off mechanism cannot remove the heat from the wire quickly enough to maintain the temperature in the wire. The wire then quickly overheats and fuses. This mechanism produces a current-limiting fusing action which is more than adequate to prevent the draining of the power source and fault current damage of the system.

4.3.7 Fault Protection

Protection of the load when a load fault occurs is a requirement for most power systems. For a 1-MW system that has an allowable fault energy of a few tens of joules, the fault protection circuitry must be triggered within a few tens of microseconds after a load fault occurs. This places a constraint on the speed of the trigger circuit. Fault protection requirements of this type are not unusual and a number of methods can provide the required fault protection. One of these is discussed in Section 4.4.

4.3.8 Reliability

Reliability is clearly important in a system that is in space and, as a result, is expensive and difficult if not impossible to repair. In some of the applications discussed for this program, even a small amount of system downtime is not acceptable; i.e., system availability must be 100%. The reliability of a system that is beyond the current state of the art and that requires components that have never been built is difficult to gauge. The approach taken to maximize reliability and availability is to use as few components as possible, and to use passive components as much as possible. The designs of all components and subsystems were performed with reliability in mind.

4.3.9 System Hardness

This system must operate in a very harsh environment. Depending on the particular application, the ambient environment may include any or all of the following: high radiation levels (ambient and weapon-generated), rapid temperature cycling, intense vacuum UV flux, high-velocity debris (ambient and weapon-generated), low-density plasma, free radicals such as oxygen and chlorine, and local pollution from the rest of the spacecraft. The power converter must be hardened against these threats in order for it to be available when needed. The approach to minimizing problems caused by the environment is to use intrinsically hard components to make up the system and to position the system in the spacecraft in a location that will minimize exposure to the threats.

Figure 4.4.1-1. Block diagram of the resonance transformer-based system.

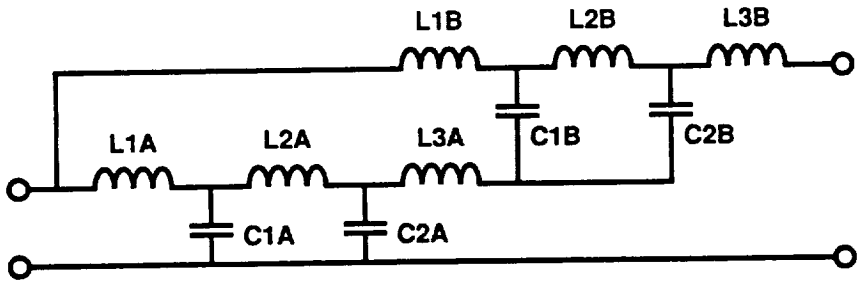

a) Cascaded ladder connected resonance transformer

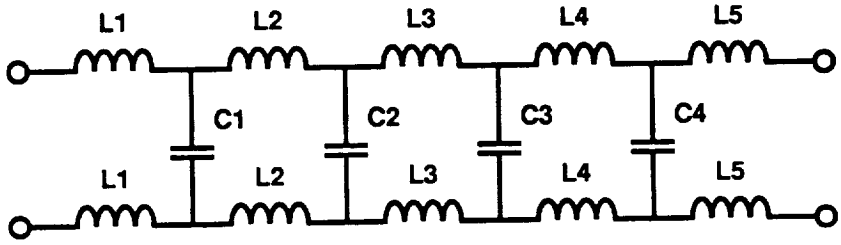

b) Symmetric series connected resonance transformer

Figure 4.4.3-1. Cascaded ladder-connected and symmetric series-connected two-stage resonance transformers.

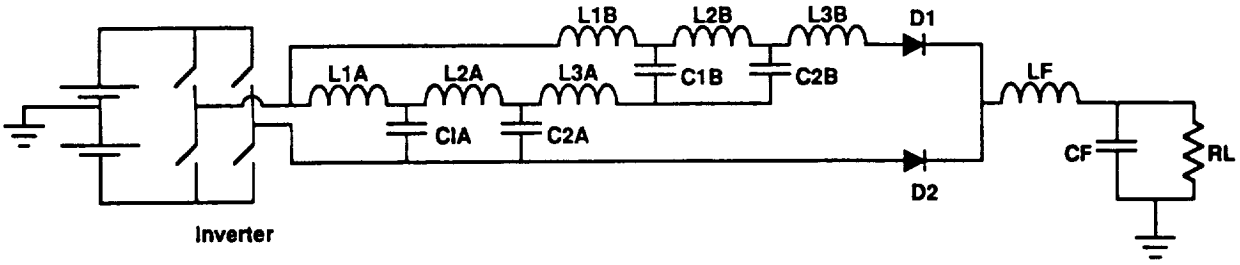

Figure 4.4.3-2. Cascaded ladder-connected circuit with diodes and filter (simplified).

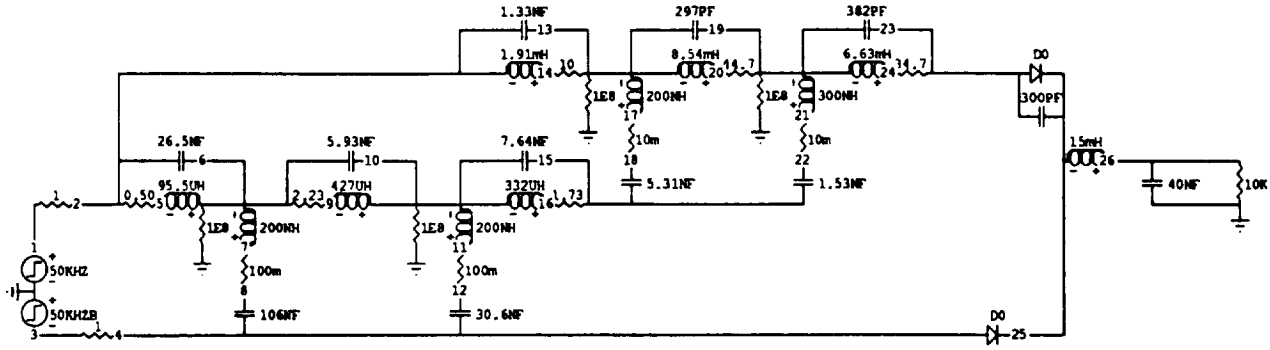

Figure 4.4.3-3. Cascaded ladder-connected system simulation circuit.

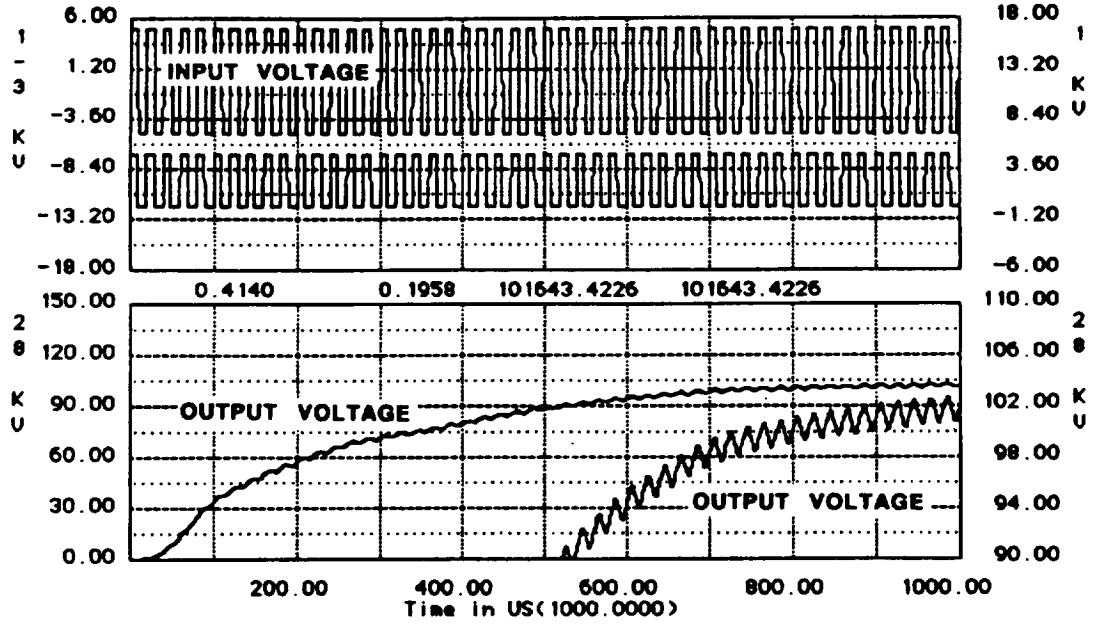

Figure 4.4.3-4. Cascaded ladder-connected system simulation circuit results.

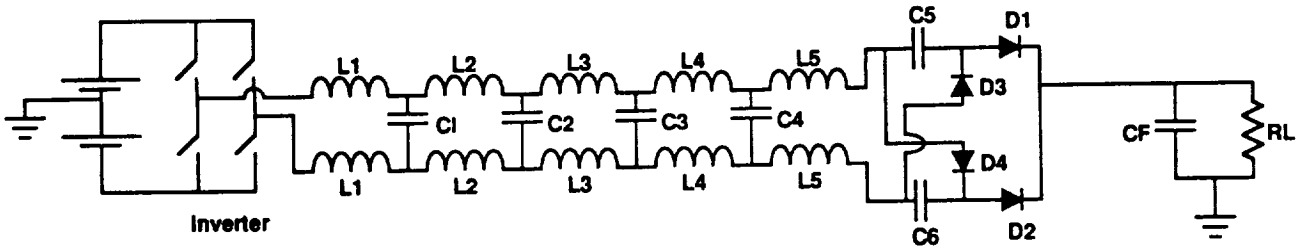

Figure 4.4.3-5. Symmetric series-connected resonance transformer-based system with capacitive voltage multiplier output.

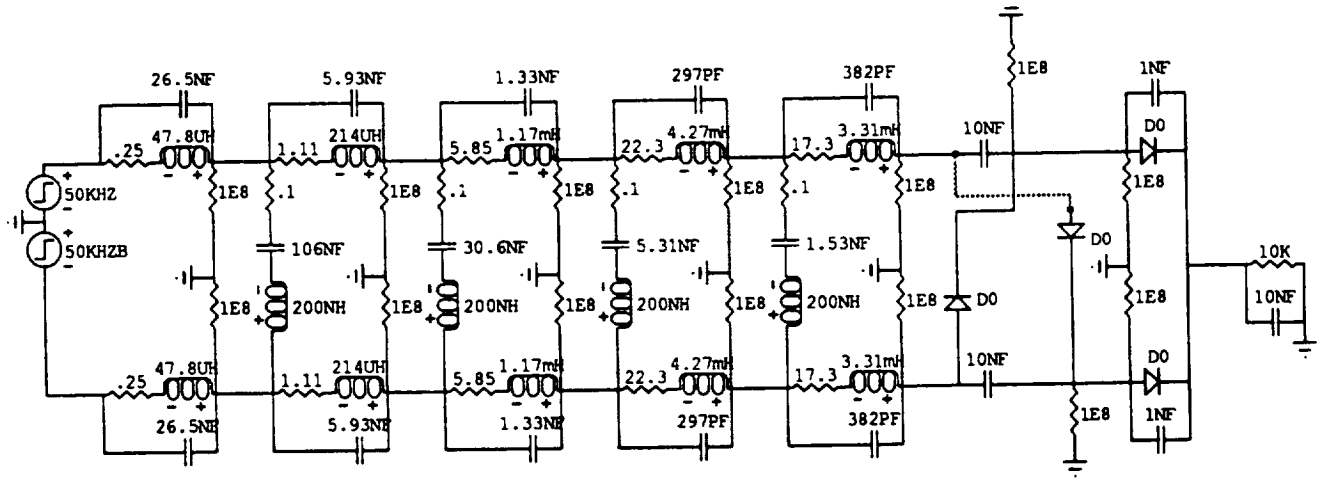

Figure 4.4.3-6. Symmetric series-connected resonance transformer-based system simulation circuit.

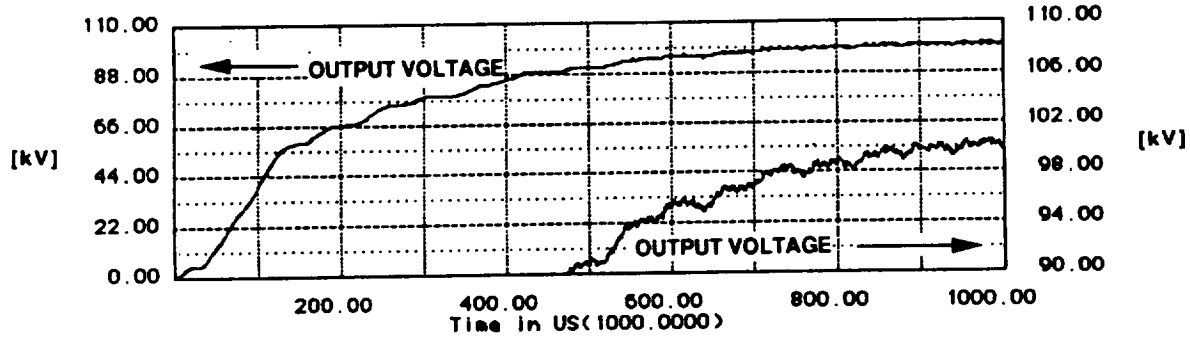

Figure 4.4.3-7. Symmetric series-connected resonance transformer-based system simulation circuit results.

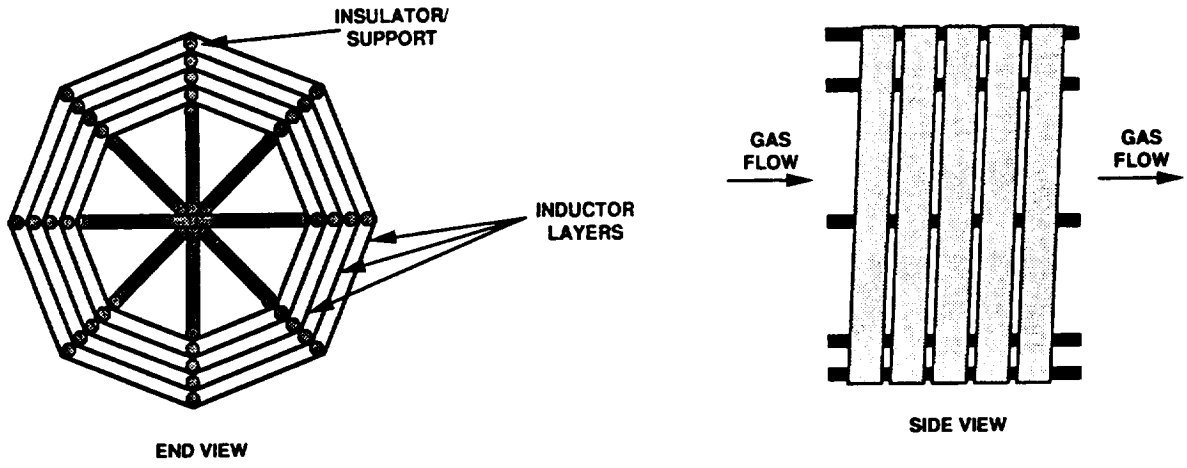

Figure 4.4.3-8. Resonance transformer inductor sketch.

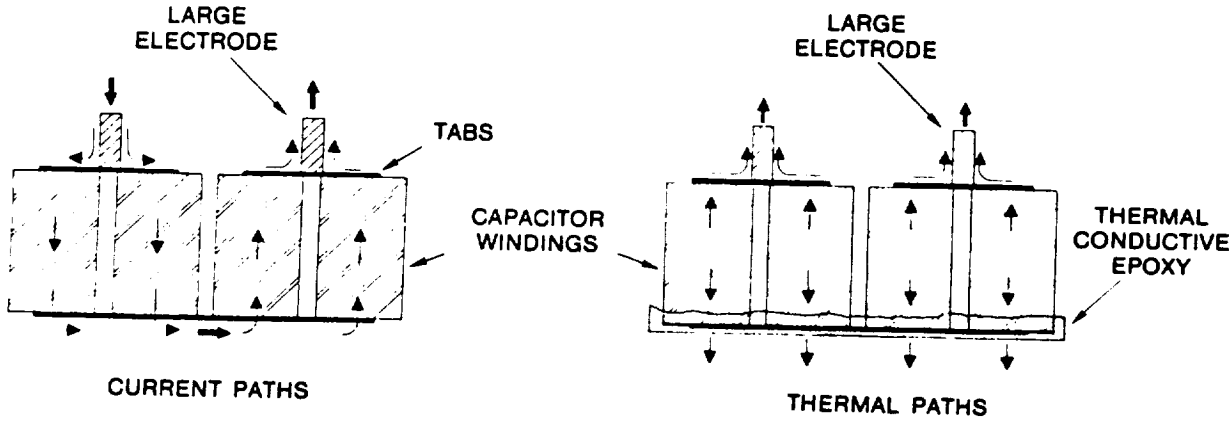

Figure 4.4.3-9. Parallel winding to divide current and thermal paths.

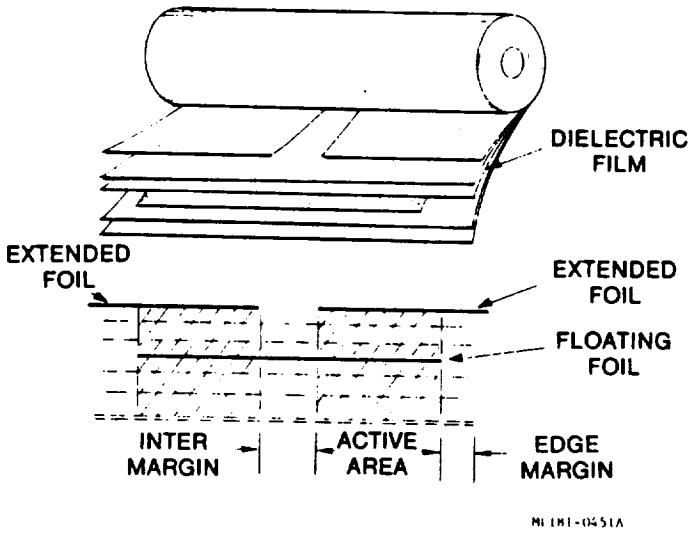

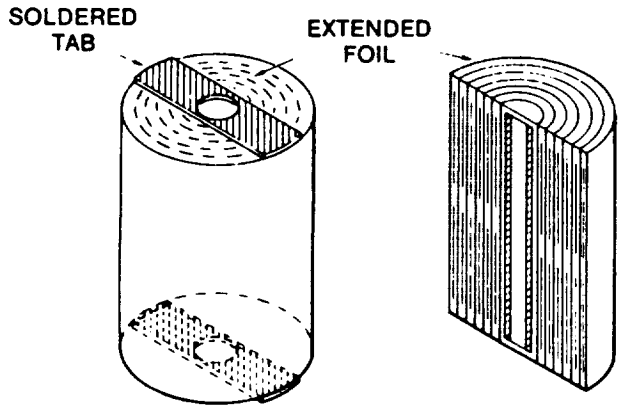

Figure 4.4.3-10. Winding detail.

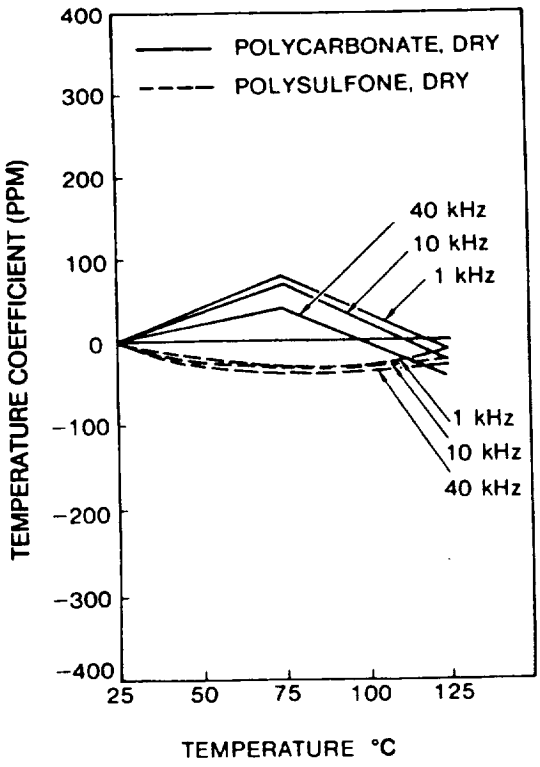

Figure 4.4.3-12. Temperature coefficient of capacitance vs. temperature.

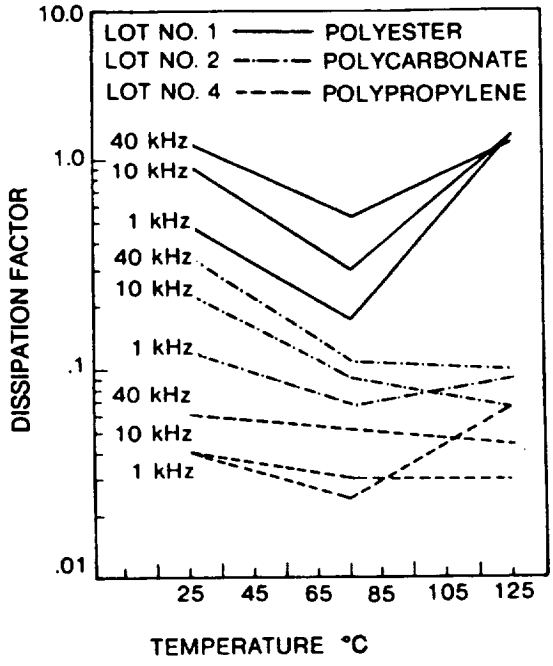

Figure 4.4.3-13. Temperature coefficient of dissipation factor.

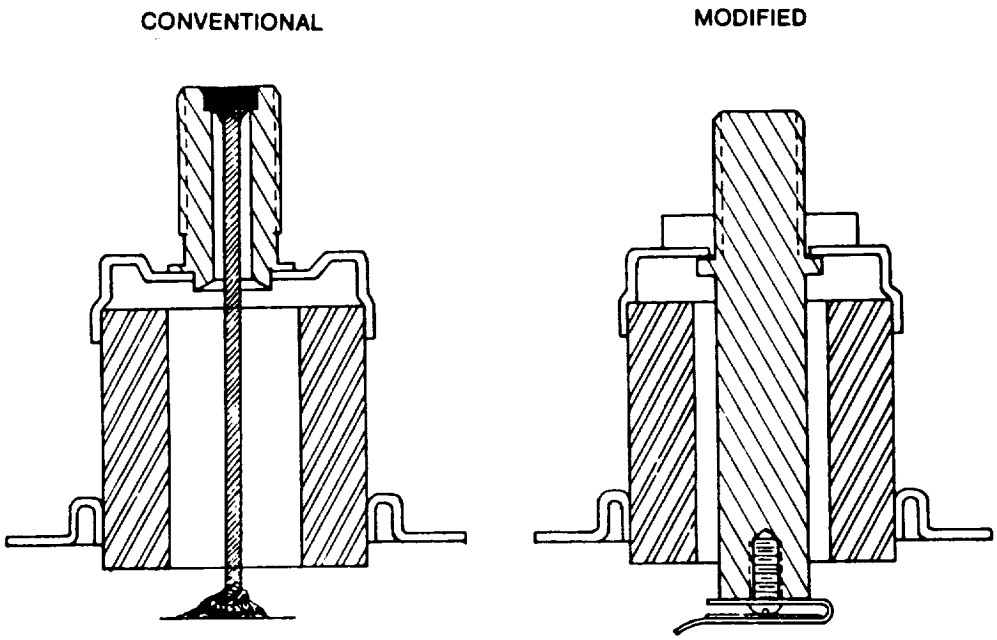

Figure 4.4.3-14. Electrode insulator assemblies.

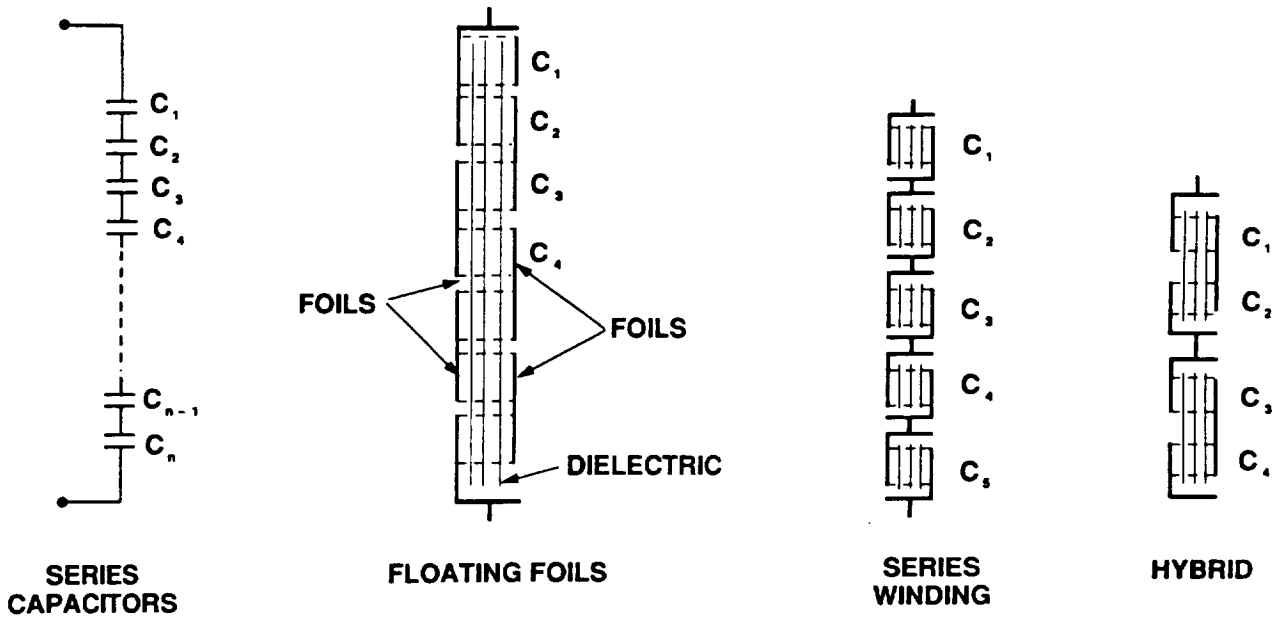

Figure 4.4.3-15. Series capacitor constructions.

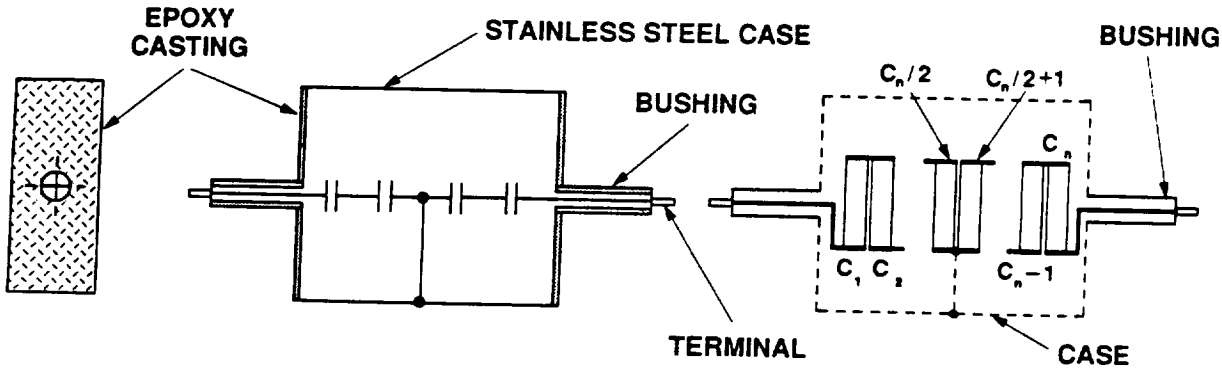

2 BUSHINGS CENTER TAPPED TO CASE
WELDED THIN STAINLESS STEEL CASE FOR HERMETIC SEAL
INTERNAL INSULATION TO EACH END FOR HALF VOLTAGE
OVERALL WEIGHT REDUCED

Figure 4.4.3-16. Center-tapped capacitor.

Summary. The capacitor specifications for the GE Super-Resonance Power System and the Maxwell Resonance Transformer Power Circuit were thoroughly investigated. The design impact of the required high power density, along with the associated high currents and power losses, was studied. Initial designs for each of the capacitors were prepared and the sizes and weights estimated. The weight objectives of the program can be met using improved existing materials together with new technology that has been developed recently at Maxwell. Center-tapped cases were used in some of the designs, which, although requiring two bushings per can, allow use of smaller bushings for reduced overall capacitor weight. Another advantage of center tapping is that it provides an additional cooling point on the capacitor for thermal management. The specific weights have been improved considerably over the previous designs developed for NASA.

4.4.4 Rectifier and Voltage Multiplier

The rectifiers for the output of the resonance transformer are also made by Harris/GE-CRD. They are very similar to the inverter in construction, with the exception that more devices are used in series. The device details are discussed in Section 2. The cascaded ladder-connected resonance transformer system requires two 240-kV diode stacks and the series-connected resonance transformer system requires two 140-kV stacks and two 70-kV stacks, so the total number of devices for the series-connected system is actually less than that for the cascaded ladder-connected system. The rectifier stacks for the voltage multiplier are comparable in size and weight to a full-wave rectifier bridge at this voltage. The voltage multiplier capacitors are very similar to the filter capacitor (discussed in Section 4.4.6).

4.4.5 Regulator

The regulator for the resonance transformer-based system is necessary to reduce the ripple of the output voltage from 1% to 0.25%. Control of the output voltage of the resonance transformer by changing the inverter frequency and by changing the duty cycle of the inverter (pulse width modulation) were investigated. Both of these techniques were found to be effective, as shown in Figures 4.4.5-1 and 4.4.5-2. Figure 4.4.5-1 illustrates control by changing the switching frequency of the inverter. The gain profile of the resonance transformer is not flat in the neighborhood of the optimal operating frequency, so by changing the frequency, the gain is changed and the output voltage is correspondingly changed.

In Figure 4.4.5-2, the effect of changing the duty factor of the inverter switches is illustrated. This method of control requires switching at points far away from current zeros, but the MCT inverter switches are uniquely capable of switching under these conditions.

One problem is common to both of these control schemes: Because of the multiple stages of the resonance transformer, there is a large time delay (phase shift) between the application of control to the inverter and the desired change to the output occurring. This places an upper limit on the frequency response of this type of control that will always be less than the operating frequency of the circuit. This type of control can be used to control the effects of source variations and other slow processes, but it is unsuitable for eliminating the output ripple.

In many power supplies requiring very low ripple, a series regulator is placed directly before the output to the load. This circuit senses the load voltage and controls a transistor or vacuum tube in series with the load such that the transistor or tube drops the excess voltage that otherwise would be applied to the load. The frequency response of this type of regulator is limited only by the speed of the control loop. For a 1-MW power system, 1% ripple corresponds to 10 kW that must be dissipated by the series regulator. This will require (1) an array of linear semiconductor devices, which will be difficult to control adequately and will be heavy,

or (2) a vacuum tube, which will require an isolated power supply and control electronics and which will also be heavy.

A third option is a regulation scheme developed by Maxwell (Figure 4.4.5-3). The regulator consists of a number of parallel combinations of FET switches and resistors in series with the load. The switches place the resistors in series with the load and remove them to control the load voltage. The minimum number of switch/resistor combinations required is determined by

$$n = (\text{input ripple voltage})/(\text{output ripple voltage})$$

where n is the number of switch/resistor combinations. The power dissipation per resistor is determined by

$$P_R = P_{out} * (\text{input ripple voltage})/(V_{out} * n),$$

where P_R is the power per resistor, P_{out} is the load power, V_{out} is the load voltage, and n is the number of switch/resistor combinations.

The operation of this regulator is straightforward. There are two output voltage thresholds for the switch control. These correspond to the minimum and maximum allowable load voltage. Initially, all the switches are closed. When the voltage across the load reaches the upper threshold, one switch opens, placing a resistor in series with the load and lowering the load voltage to the lower voltage threshold. As the load voltage continues to climb to the upper threshold, more switches are opened until the voltage fails to reach the upper threshold. When the voltage tries to drop below the lower threshold, the switches close sequentially to keep the load voltage within the proper range. This regulator has proven to be stable in computer simulations as long as the change in voltage produced by opening or closing a switch does not exceed the difference of the upper and lower thresholds. In the case of a load fault, the switches will all close to prevent damage to the regulator.

The frequency response of this regulator depends on the number of switch/resistor combinations and how fast they can be switched on and off. Since the number of switch/resistor combinations depends upon the required regulation, a higher degree of regulation is achieved at the expense of a reduced bandwidth. For a regulator with 10 switch/resistor combinations (2 kV ripple → 200 V ripple, for example), a bandwidth of 1 MHz should be possible to achieve.

For the two systems under discussion, the switches chosen are IRFP460 FETs. These FETs are efficient, highly reliable, and can operate at greater than 1 MHz, which is necessary for effective regulation. The 20-Ω resistors will be made from 10 m of 16 AWG Nichrome wire. The power dissipation in the Nichrome is 10 W/g, which should be a safe level in view of the cooling available. The control voltage and electronics power will be picked off the output voltage, and the entire regulator assembly will float at 100 kV.

4.4.6 Filter Inductor and Capacitor

The filter inductor is similar in construction to the resonance transformer inductors, primarily for weight and cooling considerations as opposed to performance considerations. It is the largest inductor at 15 mH, and is only required in the cascaded ladder-connected system.

The filter capacitor will have the same dielectric system and similar construction as the resonance transformer capacitors (discussed in Section 4.4.3). The requirements for ac and filter capacitors are different, but in this case the best dielectric system for these two applications was the polypropylene/MIPB combination.

4.4.7 Crowbar

The crowbar switch is required to limit the fault energy in case of a load fault to a few tens of joules. It accomplishes this by sensing a load overcurrent and firing to divert the current away from the load. The same sensing circuit will close the regulator to protect it, but the crowbar switch will fire first to allow the regulator resistance to aid in diverting the fault current to the crowbar switch. The crowbar circuit with trigger is shown in Figure 4.4.7-1. A Hall probe senses an overcurrent, which changes the state of a fast comparator with a zener diode reference voltage. The output of the comparator drives a pulse transformer, which triggers a KN22B krytron switch. This switch dumps a charged 1-μF capacitor into the primary of a pulse transformer. The secondary of that pulse transformer is tied to the trigger electrode of the crowbar spark gap. When the crowbar spark gap fires, it will continue to conduct until the filter and the resonance transformer are discharged and the load is safe. This very lightweight, rugged circuit has been used in a number of systems at Maxwell. The crowbar designed for the present system will handle up to 1.5 kJ easily and can be upgraded if necessary for higher fault energies.

4.4.8 Housing, Support, and Cooling Structures

The housing, support, and cooling structures for the system are closely interrelated, with most parts functioning in one or more of the above capacities. The designs are driven by the following major requirements:

- The system is cooled with H_2 at 50 K
- The housing must be light in weight
- The housing must hold 3 atm of H_2 during system operation

The cooling requirements are determined primarily by the power dissipation of the resonance transformer inductors. The overall efficiency of the system is about 88%. Approximately 80% of these losses are in the inductors. The H_2 inlet temperature is assumed to be 50 K and the outlet temperature is 200 K. Based on a system efficiency of 88% and those inlet and outlet temperatures, the estimated H_2 inlet and outlet flow rates are 195 L/s (412 ft^3/m) and 779 L/s (1651 ft^3/m), respectively. The original design used an inlet temperature of 25 K, but there was some concern that this was too close to the phase change temperature to ensure predictable cooling and high-voltage insulation performance.

The housing is only required to hold pressure during 1000 seconds of operation, plus testing. It is very difficult to make a container that will remain sealed for the required system life of on the order of 10 years and hold pressure while remaining light in weight. Because the only time the pressurization is required is during operation, and because the hydrogen is available during the alert period leading up to system operation, on-demand pressurization is possible. This reduces the requirements for the housing. For example, pinholes caused by micrometeoroids are not an issue in a on-demand pressurized system. This means that the housing can be a non-rigid structure that inflates on demand. The hydrogen inlet to this housing is a large-diameter tube to which all the components are mounted, forming the backbone of the housing. The cooling plena connect the tube to the various cryocooled components and provide support for the inductors, the inverter, and the diode stacks. This allows cooling hydrogen to flow directly to the individual inductors and semiconductor stacks. The exhaust hydrogen then pressurizes the housing. A relief valve maintains the pressure at 3 atm.

The capacitors and the regulator are also mounted to the central tube. A septum separates the inductor volume from the capacitor volume. This, along with the small cross-

sectional area of the connections between the inductors and the capacitors, allows the capacitors to remain at a much warmer operating temperature than the inductors. The overall size of the housing is 7 ft long × 2 ft in diameter.

4.5 System Selection, Mass Efficiency, and Layout

The masses for both the cascaded ladder-connected (CLC) resonance transformer-based system and the symmetric series-connected (SSC) resonance transformer-based system have been calculated, based on careful design of the components and verification of those designs by computer simulations, and are listed in Table 4.5-1. The overall efficiency of both of these systems is estimated at 87%; 66% of the losses are in the resonance transformer inductor, 20% in the inverter, 5% in the regulator, 4% in the diodes, and the remainder in the other components. The resonance transformer inductor losses were calculated at room temperature and will be lower in the actual system due to the cooler temperatures.

Table 4.5-1

Mass Breakdown

Component	CLC (kg)	SSC (kg)
Input fuse	1.0	1.0
Input filter capacitor	2.0	2.0
Inverter	8.0	8.0
Resonance transformer capacitors	20.8	20.8
Resonance transformer inductors	12.8	16.0
Voltage multiplier capacitors	-	12.6
Diode stacks	4.0	3.3
Filter inductor	4.8	-
Filter capacitor	10.0	7.4
Crowbar circuit	1.8	1.8
Regulator circuit	5.2	2.6
Cooling plena	4.3	3.3
Component supports	1.0	1.0
Envelope	4.0	4.0
Totals	79.7	83.8

The symmetric series-connected resonance transformer-based system has performance characteristics that are superior to the cascaded ladder-connected resonance transformer-based system (Section 4.4). As a result, the symmetric series-connected resonance transformer-based system was chosen for the high-power, high-voltage, dc-dc converter. This system will meet or exceed all the specifications for this converter. A conceptual layout of the housing and the converter system together is shown in Figure 4.5-1.

4.6 Risk Areas and Risk Abatement

As with any new design, some risk is involved with this approach. Some typical system issues for space-based systems are discussed in Section 4.3. This section discusses the risks inherent to this system specifically and the plans to minimize these risks when the actual design and construction of the prototype are undertaken.

4.6.1 Resonance Transformer-Based Systems

One of the risks associated with the use of a resonance transformer-based system is that only a few systems of this type have been designed and only one has been constructed to date. However, the fact that a working model has been constructed demonstrates the validity of the concept, and reduces this particular risk to that associated with making the components to the required specifications. The small-scale testing of components (Section 4.4) indicates that the components can indeed be designed to meet the requirements for this converter. This risk will be further reduced by careful component design and further small scale testing in Phase 2 of the program.

4.6.2 Cryocooling

The main risks associated with using cryogenic hydrogen gas to cool some of the components are that (1) the capacitors cannot survive if they are cooled to the hydrogen temperature, (2) there may be materials problems with hydrogen cooling, and (3) loss of coolant can quickly lead to component damage. The first risk is mitigated by housing the capacitors in a separate volume from the rest of the components and by ensuring that the thermal conduction through the electrical connections to the capacitors is minimized. The second risk is minimized by a careful selection of materials for the system and by plating the metals with an embrittlement-resistant material if necessary, as described in Section 4.3.5. The third risk is alleviated by ensuring that the controls system shuts the power system down if coolant flow is lost or if an overtemperature occurs.

4.6.3 Semiconductors in Space

The risks of the use of semiconductor devices in space have been a topic of concern in the power community for a number of years. The degradation of semiconductor device performance over time when exposed to the ambient space environment has been documented. MCTs are new devices and have not been characterized as thoroughly as the older devices. The manufacturer of MCTs is confident that the devices can be made as hard as any other semiconductor device. If this is not possible, then other, more hardened devices such as FETs or BJTs can be used for the switches in this system. The system performance and mass will be adversely affected, but not to a large enough degree that the system is not viable without the MCTs.

4.6.4 Regulator Scheme

The regulator scheme proposed promises to be a very lightweight subsystem, but it has never been used in a power system. This means it has never demonstrated stability in a real system. However, it has proven to be very stable in circuit simulations, and the components used to make it are highly reliable. The stability of this system will also be demonstrated in a small-scale demonstration in Phase 2.

4.7 System Scalability

The 1-MW system presented above is exceptionally light in weight and has a much higher power density than that achievable with converters currently in use. One of the features of the resonance transformer-based system is that the power density increases when the output power is increased for a fixed input and output voltage. This is true for power levels up to at least the hundreds of megawatts regime, which is the largest point design of a resonance transformer-based system performed to date. To demonstrate this, a system with 10 MW output power was investigated to determine the power density at this level. The results are tabulated in Table 4.7-1.

Section 5

CONCLUSIONS

The advanced power conversion system designs evaluated during Phase 1 of this program represent an extension of dc-to-dc converter technology to well beyond the present state of the art. Different tradeoffs were necessarily invoked for the two subject designs. The present study shows that both systems can in theory meet the stringent 0.1 kg/kW power density while operating in the space environment.

The super-resonant approach developed by GE, presently being used in a product application to a power level of approximately 70 kW, has demonstrated a high level of reliability. The present study extends this technology to the 1-MW power level and also includes a new, innovative control scheme that has the potential to further enhance the reliability of operation.

The resonance transformer approach developed at Maxwell avoids the use of a high-voltage transformer through the use of a new circuit configuration employing components with proven performance where possible. This use of mature components should make the overall system very reliable.

Both system approaches will exhibit higher power density at higher power levels.

Table 5-1 compares the two systems in terms of mass, power dissipation, efficiency and enclosed volume.

Table 5-1

System Comparison

Converter Component	System Approach: Super-Resonant Mass (kg)	Super-Resonant Loss (W)	Resonance Transformer Mass (kg)	Resonance Transformer Loss (W)
Input fuse	1.0	10	1.0	5
Dc input filter capacitor	3.0	5	2.0	5
Inverter	8.0	42400	8.0	40000
Power circuit	44.0*	12236*	52.7	101400
Dc output filter capacitor	14.0	60	7.4	1
Dc output crowbar	2.0	0	1.8	0
Control electronics	0.5	-	2.6	5000
Cooling system	10.0	1000	3.3	-
Component support structure	4.5	-	1.0	-
Envelope enclosure (ft^3)	1.5 (10)	-	4.0 (22)	-
Total system	88.5	55711	83.8	146411
System efficiency	94.4%		87.2%	

*Includes the resonant inductor and capacitor, transformer and high-voltage output rectifier

Section 6

PROPOSED FOLLOW-ON ACTIVITY

6.1 Program Phase 2

GE and Maxwell Laboratories propose to develop their specific approaches conducted as parallel efforts. Both systems use an MCT-based inverter of nearly identical design. This parallel approach uses the synergy developed between GE and Maxwell and permits the development of both systems at a cost that is much less than if they were to be developed separately. Harris Semiconductor will develop one MCT module type to be used with both system approaches.

6.1.1 Phase 2A – 100-kW Proof-of-Principle Breadboard Development (One Year)

GE will develop one air-cooled, MCT-based, 100-kW super-resonant converter breadboard using a 1-MW transformer, suitable for laboratory testing. A simple form of optimal closed-loop control will be developed. Only one 1-MW transformer will be built for use with the breadboard.

Maxwell will develop one air-cooled, MCT-based, 100-kW resonance-transformer converter system and provide testing. A "bare-bones" closed-loop control will be provided.

For each system, the 100-kW proof-of-principle converter hardware shall comprise an operating breadboard sufficient to obtain any necessary data in a laboratory environment. Maxwell will be responsible for all capacitors, power supply, input fuse, resonance transformer, crowbar circuit, dummy load, and housing for both systems. GE will provide the inverter and output rectifiers for both systems. No component-level testing will be performed. Maxwell will perform all high-voltage system-level testing.

Gaseous hydrogen cooling, completion of optimal control (GE), and 1-MW breadboard hardware development are proposed for the next phase.

6.1.2 Phase 2B – 1-MW Proof-of-Principle Breadboard Development (One Year)

As with Phase 2A, GE and Maxwell Labs will continue to develop their specific approaches to be conducted as parallel efforts. Harris Semiconductor will develop one MCT module type to be used with both system approaches.

GE will develop one air-cooled, MCT-based, 1-MW super-resonant converter breadboard suitable for laboratory testing. A simple form of optimal closed-loop control will be used. The 1-MW transformer developed for Phase 2A will be utilized with the 1-MW breadboard.

Maxwell will develop one air-cooled, MCT-based, 1-MW resonance-transformer converter system and provide testing. A "bare-bones" closed-loop control will be provided.

For each system, the 1-MW hardware shall comprise an operating breadboard sufficient to obtain any necessary data in a laboratory environment. Maxwell will be responsible for all capacitors, power supply, input fuse, resonance transformer, crowbar circuit, dummy load, and housing for both systems. GE will provide the inverter and output rectifiers for both systems. Maxwell will perform all high-voltage system-level testing.

Gaseous hydrogen cooling, completion of optimal control (GE), and 1-MW brassboard hardware development are proposed for the next phase.

NASA
National Aeronautics and Space Administration

Report Documentation Page

1. Report No.	2. Government Accession No.	3. Recipient's Catalog No.
NASA CR-187116		

4. Title and Subtitle	5. Report Date
High-Power Converters for Space Applications	June 1991
	6. Performing Organization Code

7. Author(s)	8. Performing Organization Report No.
J.N. Park, GE-CRD; Randy Cooper, Maxwell Laboratories	90SRD008
	10. Work Unit No. 506-41-3F

9. Performing Organization Name and Address	11. Contract or Grant No.
Prime contractor: GE Corporate Research and Development P.O. Box 8, Schenectady, NY 12301	NAS3-25800
	13. Type of Report and Period Covered Contractor Report Final

12. Sponsoring Agency Name and Address	14. Sponsoring Agency Code
National Aeronautics and Space Administration Lewis Research Center Cleveland, OH 44135-3191	

15. Supplementary Notes

Project Manager: Ira T. Myers, Power Technology Division, NASA Lewis Research Center

Subcontractor: Maxwell Laboratories,
8888 Balboa Avenue, San Diego, CA 92123-1506

16. Abstract

Phase 1 was a concept definition effort to extend space-type dc/dc converter technology to tl megawatt level with a weight of less than 0.1 kg/kW (220 lb/MW). Two system designs were evaluate in Phase 1. Each design operates from a 5-kV stacked fuel cell source and provides a voltage step-up 100 kV at 10 A for charging capacitors (100 pps at a duty cycle of 17 min on, 73 min off). Both desig use an MCT-based, full-bridge inverter, gaseous hydrogen cooling, and crowbar fault protection.

The GE-CRD system uses an advanced high-voltage transformer/rectifier filter in series with resonant tank circuit, driven by an inverter operating at 20 to 50 kHz. Output voltage is controlle through frequency and phase shift control. Fast transient response and stability is ensured via "optim control." Super-resonant operation employing MCTs provides the advantages of lossless snubbing, r turn-on switching loss, use of medium-speed diodes, and intrinsic current limiting under load-fau conditions. Estimated weight of the GE-CRD system is 88.5 kg (1.5 ft^3). Efficiency is 94.4% and tot system loss is 55.711 kW operating at 1 MW load power.

The Maxwell system is based on a resonance transformer approach using a cascade of five L resonant sections at 100 kHz. The 5-kV bus is converted to a square wave, stepped-up to a 100-kV sin wave by the LC sections, rectified, and filtered. Output voltage is controlled with a special serie regulator circuit. Estimated weight of the Maxwell system is 83.8 kg (4.0 ft^3). Efficiency is 87.2% an total system loss is 146.411 kW operating at 1 MW load power.

17. Key Words (Suggested by Author(s))	18. Distribution Statement
light weight; high-power converters; high-voltage, high-frequency converters	Unclassified – Unlimited Subject Category 33

19. Security Classif. (of this report)	20. Security Classif. (of this page)	21. No of pages	22. Price*
Unclassified	Unclassified	139	A07

NASA FORM 1626 OCT 86

*For sale by the National Technical Information Service, Springfield, Virginia 22161